energies

MDPI

Article

Prioritizing Energy-Intensive Machining Operations and Gauging the Influence of Electric Parameters: An Industrial Case Study

Ardamanbir Singh Sidhu [1], Sehijpal Singh [2], Raman Kumar [2,*], Danil Yurievich Pimenov [3] and Khaled Giasin [4]

[1] Department of Mechanical Engineering, I. K. Gujral Punjab Technical University, Jalandhar 144603, India; aol.ardaman@gmail.com
[2] Department of Mechanical and Production Engineering, Guru Nanak Dev Engineering College, Ludhiana 141006, India; sehijpalsingh@yahoo.co.in
[3] Department of Automated Mechanical Engineering, South Ural State University, Lenin Prosp. 76, 454080 Chelyabinsk, Russia; danil_u@rambler.ru
[4] School of Mechanical and Design Engineering, University of Portsmouth, Portsmouth PO1 3DJ, UK; khaled.giasin@port.ac.uk
* Correspondence: sehgal91@yahoo.co.in; Tel.: +91-9855100530

Abstract: Increasing the energy efficiency of machining operations can contribute to more sustainable manufacturing. Therefore, there is a necessity to investigate, evaluate, and optimize the energy consumed during machining operations. The research highlights a method employed to prioritize the most energy-intensive machining operation and highlights the significance of electric parameters as predictors in power estimation of machining operations. Multi regression modeling with standardized regression weights was used to identify significant power quality predictors for active power evaluation for machining operations. The absolute error and the relative error both decreased when the active power was measured by the power analyzer for each of the identified machining operations, compared to the standard power equation and that obtained from the modeled regression equations. Furthermore, to determine energy-intensive machining operation, a hybrid decision-making technique based on TOPSIS (a technique for order preference by similarity to ideal solution) and DoM (degree of membership) was utilized. Allocation of weights to energy responses was carried out using three methods, i.e., equal importance, entropy weights, and the AHP (analytical hierarchy process). Results revealed that a drilling process carried out on material ST 52.3 is energy-intensive. This accentuates the significance of electric parameters in the assessment of active power during machining operations.

Keywords: machining operations; electric parameters; active power; active energy; specific energy consumption; energy efficiency; TOPSIS; entropy weight; AHP

Citation: Sidhu, A.S.; Singh, S.; Kumar, R.; Pimenov, D.Y.; Giasin, K. Prioritizing Energy-Intensive Machining Operations and Gauging the Influence of Electric Parameters: An Industrial Case Study. *Energies* **2021**, *14*, 4761. https://doi.org/10.3390/en14164761

Academic Editor: Dimitrios A. Georgakellos

Received: 1 July 2021
Accepted: 3 August 2021
Published: 5 August 2021

1. Introduction

Manufacturing activities can negatively impact the environment. It is one of the major consumers of electricity. Electricity production and heat contribute to CO_2 emissions, especially the production of electricity through fossils fuels like coal. Due to Covid-19, there was an unprecedented decline in emissions in 2020. Worldwide CO_2 emissions from the electricity sector reduced by almost 450 million tons in 2020 [1]. This was mainly due to the reduction in industrial production. Worldwide energy demand dropped by 3.8% in the first quarter of 2020 compared with the first quarter of 2019. As a result, annual energy demand in 2020 decreased by 6%. The reduced use of coal amounted to 1.1 Gt of reductions in CO_2 emissions. This highlights that the increase in manufacturing activity and its decrease in the lockdown period due to the coronavirus pandemic directly affected the growth and decline of CO_2 emissions [2,3].

The IEA (International Energy Agency) Global Energy Review 2021 assessed that emissions of CO_2 are likely to increase by 5% to 33 billion tons. Global energy demand is expected to increase by 4.6% in 2021. The electricity sector is expected to contribute to 75% of this increase. Unless tangible steps are taken to curb emissions of CO_2, the situation in 2022 may become alarming [2,3]. It is a clear warning that enough is not being done to introduce clean energy technologies. We face an immense challenge in reforming the worldwide energy system. Therefore, there is a need to inculcate machining practices that limit electrical energy consumption and promote a green environment, thus highlighting the need for this research.

Review papers provide great insight into the work done to improve the energy efficiency of machining processes. For example, Zhang et al. [4] focused on theoretical and experimental models in the preview of energy efficiency of machine tools, Yoon et al. [5] reported on energy-saving strategies in the case of machine tools, Zhou et al. [6] researched in the field of cutting energy models based on machining processes, and Zhao et al. [7] concentrated on the optimization of energy components, process constraints, and improvements in auxiliary system efficiency.

The literature review indicates that research in energy conservation of machining processes started way back in 1994 when Bayoumi and Hutton [8] applied specific cutting energy to measure energy efficiency in the milling process. Draganescu et al. [9] stipulated numerical models for specific energy consumption and energy efficiency at the spindle level. Gutowski et al. [10] reported that the energy consumed by the cutting process accounts only for 20% of the total energy consumed by the machine tool. A theoretical model for the power consumption of a machine tool was put forward and the concept of specific energy consumption (SEC). Li and Kara [11] proposed an empirical SEC model in the turning process on a CNC lathe. The model encompassed coefficients related to workpiece materials and machine tools, along with material removal rate (MRR). He et al. [12] stated that machine tools usually function at an efficiency of less than 30% and have a high possibility for energy saving and efficiency improvement.

The SEC model introduced the milling process and considered the effect of change in spindle energy due to different cutting conditions [13]. A generalized SEC put up a model for automated machine tools in the milling process [14]. The production of machine tools and energy efficiency were solved with the help of scheduling and electricity utilization with a hybrid genetic algorithm. This method could diminish prices, minimize greenhouse gas emissions, and save energy [15]. Velchev et al. [16] set up an energy consumption model for the turning process and optimized the machining parameters. The main barrier faced in getting enhanced industrial energy efficiency is the mindset and attitude of manufacturing unit owners toward sustainable development and product manufacturing. The 11 key hurdles to making more sustainable and low-carbon manufacturing units were discussed [17]. Zhao et al. [18] broadened the model proposed by Li et al. [13] for the SEC for the turning process by considering the coolant pump's unloaded spindle power and power accompanied by standby and cutting power. Sealy et al. [19] measured the energy consumption of the machine tools at the cutting, spindle, and machine tool levels. Zhou et al. [7] broadened the Gutowski [10] and Li [11] models by considering the outcome of the speed of the spindle upon power utilization in the milling process. Other research focused on machining process-level energy. For example, Hu et al. [20] examined the machine tool's variable and fixed energy utilization states. They recommended an online method for checking the energy efficiency and energy utilization ratio of the machine tool.

Many researchers set up empirical models based upon the different working states of the machine tool. For example, an energy model was presented while considering tool-set time, tool change, MRR, and embodied energy of the cutting tool [21]. The energy consumption of different machine tools was observed on the basis of each machine tool's size and technical features [22]. The total energy in the milling process was estimated, taking into consideration different tool paths. The total energy consumed was the aggregate of

energy consumed for each state, e.g., basic state, tool change spindle rotation, coolant, feed motion, and the cutting state [23]. The machining energy was modeled on the basis of rapid transverse, spindle acceleration, and material removal states [24]. The variation in specific cutting energy was studied using undeformed chip thickness, tool wear, cutting tool nose radius, and dry and flood coolant, assuming that the tip energy was 25% of the total energy demand. The optimum feed rate level helped the study achieve a 72% reduction in tip energy, amounting to about an 18% reduction in total direct energy. It was pointed out that tool wear increases the specific energy coefficient, and the flood-cutting environment decreases the specific energy coefficient. Nose radii do not significantly alter the specific energy demand [25]. A model for energy consumption was suggested in the milling process based on machine tool constituents such as the spindle, feed axes, coolant pump, ATC, and chip conveyor. The spindle power was further modeled as a linear function of spindle speed. The axis feed power was modeled as a linear function of the feed rate. Lastly, the energy consumed in the cutting process was estimated as a difference between the total energy consumed and the energy consumed during the air cut [26].

The machine tool's total energy utilization was computed considering the power model and operation time for each machine tool component such as the spindle, tool changer, axis, coolant, chip conveyor, and clamping [27]. A specific energy consumption model was presented for material removal during the milling process, considering actual cutting energy and air-cutting energy [28]. A therblig-based value stream model was proposed. The therblig approach is built on the micro motions in the machine tool. Thus, the machining operations are split into series of small energy-consuming machine tool motions. This approach helps to analyze the energy consumption of the basic motions of the machine tool [29]. The idle, cutting, and tool change states were considered and put forward a model of direct machining energy. The model included embodied energies of the cutting tool and the coolant as indirect energy [30].

Few studies focused on improving energy efficiency. Instead, experiments were performed to conserve energy considering a weight reduction of moving parts of the machine tool by introducing lotus-type porous carbon steel, energy-saving by reducing standby time, use of an optimum-capacity coolant pump, and the influence of tilting angle on machining energy [31]. In addition, many researchers worked on the optimization of the machining parameters for a decrease in energy consumption. The modification of machining variables led to improved energy efficiency and reduced energy consumption. A higher cutting value led to diminished power of drilling, face, and end milling, but constraints of surface quality and life of tool must be considered. An adaptive pecking cycle also led to the lower power consumption of deep hole machining [32]. The dry milling process was performed on medium carbon steel C45 with input responses of cutting speed, feed, depth of cut, and radial depth of cut, and optimized output responses such as carbon emissions, surface roughness, and MRR [33]. The dry turning process was performed on AISI 1045 steel and optimized with the help of grey relational analysis for cutting power and surface roughness (Ra) [34]. The machining process of grooving was observed under dry conditions on AISI 4340 steel and considered an additional input response factor of the hardness of the material; the MRR and tool wear carbon emissions were optimized with the help of the fuzzy method [35]. Turning experiments were performed on alloy steel with input parameters of cutting speed, feed, depth of cut and nose radius, optimized energy efficiency, active energy consumption, and power factor during the machining process with the help of Taguchi and ANOVA [36]. Kumar et al. [37] researched the wet turning of EN 353 alloy and optimized the output response parameters of energy efficiency, active power consumption, active energy consumption, MRR, Ra, and power factor with the help of the Taguchi and TOPSIS methods. The effect of longitudinal ultrasonic vibrations and minimum quantity lubrication on the drilling force, burr height, and Ra was identified with the help of the RSM technique, showing that the most influential factors were the feed rate, vibration amplitude, and spindle speed [38]. A multi-objective optimization

was performed on Ra, MRR, and SEC based on grey relational analysis while turning AISI 304 austenitic steel [39].

The literature review reveals specific terms used to express the energy efficiency of machine tool and machining processes. The energy utilization ratio is the ratio of the energy utilized for actual cutting or machining the workpiece to the total energy consumed by the machine tool. Researchers [19,28,37] utilized the concept of instantaneous energy efficiency in their research. This is the ratio of the power used during the cutting or machining process to the total power consumed by the machine tool at that instant. Researchers [9,20] also used SEC in their work, which can be described in three stages at the process, spindle, and machine tool levels. At the process level, it is defined as the ratio of energy consumed for material removal or the machining process to the volume of the material removed; alternatively, it is the ratio of the power consumed to the material removal rate. At the spindle level, it is the energy consumed by the spindle motor during machining to the volume of the material removed. At the machine tool level, it is the ratio of the volume of the material removed. A few authors used the concept of relative energy efficiency in their works [30,40] for energy benchmarking. This is the ratio of the minimum energy required to remove the material to the actual energy consumed to remove the material.

1.1. Research Gaps Based on Literature Review

The literature survey revealed that the research in the field of energy efficiency of machining processes has mainly been dedicated to building up empirical models for evaluating energy consumption. The empirical models obtained use coefficients and constants that depend on the machine tool's nature, the nature and composition of the workpiece, and the cutting tool. Such constants can be determined from experimental data only. However, there is a current need to evaluate energy or power consumption directly with the help of devices such as power loggers or power quality analyzers rather than empirical models. The literature review also revealed that most research has been conducted on machining processes such as turning or milling for parametric optimization. However, it is better to investigate, evaluate, and optimize machining processes that are energy-intensive. Moreover, the studies conducted previously revealed that electric parameters and their impact on power consumption have not been analyzed. Hence, there is a need to investigate the electric parameters and prioritize the most energy-intensive machining processes. The "most energy-intensive" term refers to the machining operation consuming maximum energy. It is judged on the basis of not only a single condition of energy consumption but also criteria such as specific energy consumption and energy efficiency.

1.2. Research Questions and Intended Contribution of the Study

Considering the research gaps mentioned above, the study addressed the following research question:

> *"Do we need to identify the electric parameters and prioritize the most energy-intensive machining processes?"*

The answer to this query is yes; this study can fill the gap of nonavailability of a systematic methodology to prioritize the most energy-intensive machining process. Research on the shop floor of an industry poses a significant challenge. However, it is one way to get hands-on knowledge and awareness about the industry's real challenges. This increases the chances of implementation of the results of the research by the industry. The time restrictions for conducting experiments represent one of the challenges faced. The production time of the industry may be affected. Halting one machine tool to perform experiments may stop the entire production line. However, actual conditions can be monitored and improved only when a real situation is observed on the shop floor. This helps to identify the impact on the quality of power being supplied to the given machine tool

due to the working of other machine tools in the vicinity and the impact of electric parameters on power consumption. An empirical study or theoretical research is of no use unless it is meaningful and practical for the industry. This study intends to contribute the methodology to any industry to find significant electric parameters and identify the most energy-intensive machining operations. Hence, the investigation laid down several research objectives, described below.

1.3. Research Objectives

Considering the research gap and intended contribution, the study based its investigation upon the premises of the following research objectives:

- To investigate the significant electric parameters and to analyze their impact on power consumption.
- To ascertain a methodology to identify and prioritize the most energy-intensive machining processes.

The rest of the paper is organized as follows: Section 2 describes the materials and methods. Then, it identifies methods used to achieve the research objectives, followed by explaining the materials and machine tools used for experimentation. Section 3 deals with an investigation of significant electric parameters with the help of multiple regression modeling and determination of their impact on active power consumption. Section 4 includes the hybrid decision-making methodology and its application to prioritize energy-intensive machining operation, as well as a discussion of the results, followed by the conclusions in Section 5.

2. Materials and Methods

A case study was conducted to prioritize energy-intensive machining operations and gauge the influence of electric parameters. Firstly, the research team identified the manufacturing industry for performing experiments. As a result, Auto International was selected in the industrial hub of Ludhiana, Punjab, India. It is located in Kohara, a place near the industrial town of Ludhiana. The main reason for choosing this industry was the willingness and cooperation of the management of the industry to extend their facility for experimentation despite the busy schedule of the shop floor. In addition, the industry management was interested in the outcome of the investigation and looked forward to the energy conservation of their machining operations. Next, the research team assessed the various machining operations in the concerned industry's machine shop. The identified operation consisted of different machining operations to accomplish the final product. The details of the specified machining operation are shown in Figure 1.

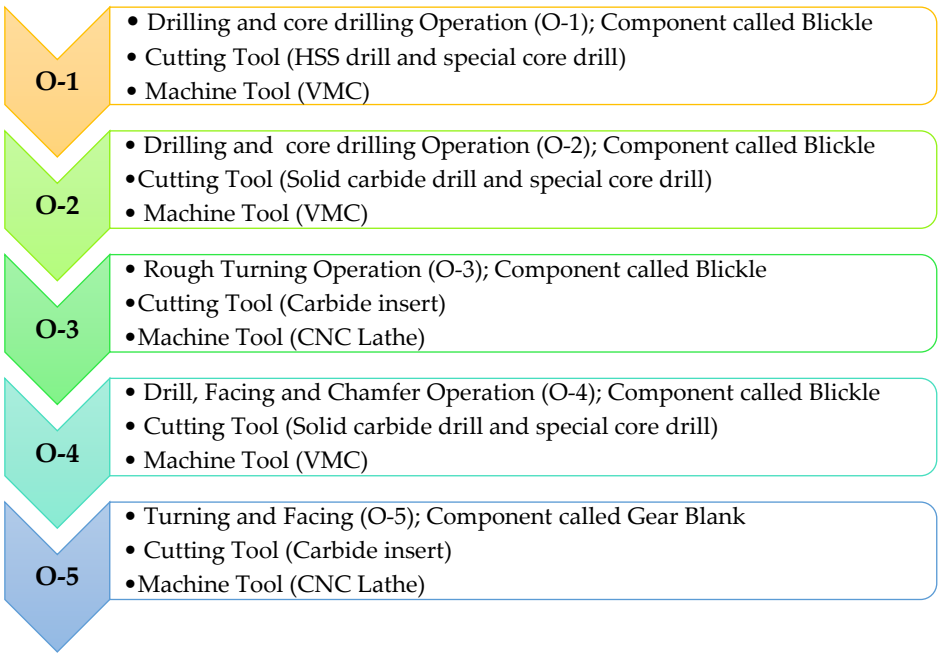

Figure 1. Machining operation details identified for study in the machine shop of the industry.

A component called a Blickle (shown in Figure 2a, used as a component in airport trolleys) was machined on a vertical milling machine (VMC). The first four operations (O-1 to O-4) shown in Figure 1 were performed on the Blickle. Operation O-1 involved drilling with an HSS drill and special core drill. Operation O-2 consisted of drilling with a solid carbide drill and special core drill. Operation O-3 involved rough turning with a carbide insert. Lastly, O-4 consisted of drilling, facing, and chamfering with a solid carbide drill and special core drill. A Gear Blank (Figure 2b, used as a component in tractor gears) was machined as the workpiece for O-5; its machining was completed on a CNC lathe. Operation O-5 involved the turning and facing of the Gear Blank with a carbide insert. The details of the workpiece, including the Blickle and Gear Blank, are shown in Table 1. The cutting tools utilized for machining operations from O-1 to O-5 and their materials and particulars are shown in Table 2. The details of cutting parameters for each operation are shown in Table 3. The specifications of the machine tools used are presented in Table 4. Figure 3a shows the power logger, and Figure 3b shows the connections of the power logger with the main power supply.

(**a**) Blickle (**b**) Gear Blank for turning

Figure 2. Identified components under study.

Table 1. Details of the workpiece.

Component Blickle for O-1 to O-4	
Workpiece material	Mild steel grade: DIN: ST52.3
Percentage composition	C: 0.207–0.22, Mn: 1.04–1.6, Si: 0.240–0.5, P: 0.033–0.035, Al: 0.038, and rest Fe
Surface Hardness	149/167 BHN
Grain size	6.5 to 7.0
Micro Structure	Pearlite + ferrite
Applications	Manufacturing of automobile parts, airport trolley parts
Component Gear Blank for O-5	
Workpiece material	20MnCr5 steel or EN 10084-2008
Percentage composition	C: 0.17–0.22, Si_{max}: 0.4, Mn: 1.1–1.4, Cr: 1–1.3, P_{max}: 0.035, S_{max}: 0.035
Applications	Auto parts, tractor parts

Table 2. Cutting tools, materials, and particulars.

Operation	Cutting Tool	Technical Particulars
O-1 Drilling	HSS drill; Make: ITM	Diameter Φ 16.0, flute length 110 mm, point angle 140°, number of flutes 2
O-1 Core Drilling	Special core drill (solid carbide) with SECO inserts; Namoh Tooling's	Flute length 85 mm, diameter Φ 17.75, tool with two fine boring inserts SECO make SCGX060204P2
O-2 Drilling	Solid carbide drill; Namoh Tooling's	Diameter Φ 16, point angle of 140°, coating of TiAIN, flute length 100 mm, shank length of 50 mm, external cooling
O-2 Core Drilling	Special core drill (solid carbide) with SECO inserts; Namoh Tooling's	Flute length 85 mm, diameter Φ 17.75, tool with two fine boring inserts SECO make SCGX060204P2
O-2 Chamfer	SECO insert	TCMT110204-F1-TP1501, chamfer at angle 45°
O-2 Facing	SECO insert	SCGX060204P2
O-3 Rough Turning	SECO carbide insert	WNMG060408-M5-TP1501
O-3 Facing	Facing insert; SECO Make	ONMU0900520 ANTN-M13-F40M
O-4 Drilling	Special carbide drill Namoh Tooling	Flute length 50 mm, point angle 140°
O-4 Chamfer	SECO insert	TCMT110204-F1-TP1501 chamfer at angle 45°
O-4 Facing	SECO insert	SCGX060204P2
O-5 Turning and Facing	SECO carbide insert	WNMG060408-M5-TP1501

Table 3. Cutting parameters for machining operations.

Machining Operation	Cutting Parameters Details
O-1	Drilling and Core Drilling-1: (on VMC) Drilling-1 (HSS drill): External diameter of workpiece 30 mm Hole diameter in drilling: 16 mm, Spindle RPM 450 Incremental peck drilling 15 mm of peck length, Feed rate 70 mm/min, the actual depth of the hole 77 mm Core drilling: Core diameter 17.8 mm, Spindle RPM 1200, Feed rate 120 mm/min
O-2	Drilling and Core Drilling-2: (on VMC)

	Drilling-2 (Solid carbide drill): External diameter of workpiece 30 mm Hole diameter in the drilling 16 mm, Spindle RPM 1050 Incremental peck drilling 10 mm of peck length, Feed rate 125 mm/min, The actual depth of the hole 77 mm Core drilling: Core diameter 17.8 mm, Spindle RPM 1200, Feed rate 120 mm/min
O-3	Rough Turning: (on CNC) External diameter of rough turning 35 mm, Final diameter 31.4 mm, depth of cut of 1.8 mm, feed of 0.18 mm/rev, Cutting speed 31 m/min, Length of cut 105 mm
O-4	Drilling and Chamfer, Facing: (on VMC) Facing: Spindle RPM 1500, Feed rate of 200 mm/min Drilling: Drill diameter 14 mm, Spindle speed 1500 RPM, Incremental peck drilling Peck length 8.2 mm, Hole depth 10.5 mm Chamfer: Spindle RPM 2000, Feed 150 mm/min, 1 × 45°
O-5	Turning and Facing: (on CNC) Turning: Final outer diameter obtained 133.4 mm, Length of cut 19.1 mm, depth of cut 1 mm, Feed 0.18 mm/rev, Cutting speed 168 m/min Facing-1: Outer diameter 133.4 mm and inner diameter 105 mm, faced through the depth of 1 mm. Feed 0.18 mm/rev, cutting speed 150 m/min Facing-2: Outer diameter 68 mm and inner diameter 52.78 mm, faced through the depth 1 mm, Feed 0.18 mm/rev, cutting speed 76 m/min

Table 4. Technical specifications of machine tool used.

Description	Units	VMC BFW/V-4 BT-40	CNC LATHE BFW RHINO (2550)	CNC LATHE JYOTI (DX-100)
CNC System	-	Fanuc 01-MF	Fanuc (B-6i) 828D	Siemens
Spindle Motor Power	kW	7.5 (Cont.) 11 (Int.)	11 15	7 10.5
Spindle Speed	rpm	8000	2000	4000
Table *X*-Axis	mm	600	200 (cross)	360
Saddle *Y*-Axis	mm	450	-	-
Spindle *Z*-Axis	mm	500	625 (longitudinal)	200
Axis Drives Feed Rate	mm/min	1–10,000	20 Rapid feed (*X* and *Z*) axis	24 Rapid feed (*X* and *Z*) axis
Ball screw Día × Pitch	mm	32 × 16	32 × 10 (*X*-axis) 40 × 10 (*Z*-axis)	32 × 10
Table Clamping Area	mm × mm	450 × 900	-	-
ATC (No. of Tools)	-	24	8/12	5
Accuracy Positioning	mm	±0.007	±0.007	±0.007
Accuracy Repeatability	mm	±0.005	±0.005	±0.005
Power Supply		3-Phase, 415 V, 50 Hz	3-Phase, 415 V, 50 Hz	3-Phase, 415 V, 50 Hz
Total Machine Power	KVA	18	16	
Chuck Size	mm	-	250	170
Std. Turning Diameter	mm	-	350 (max)	100
Max. Turning Length	mm	-	200	200

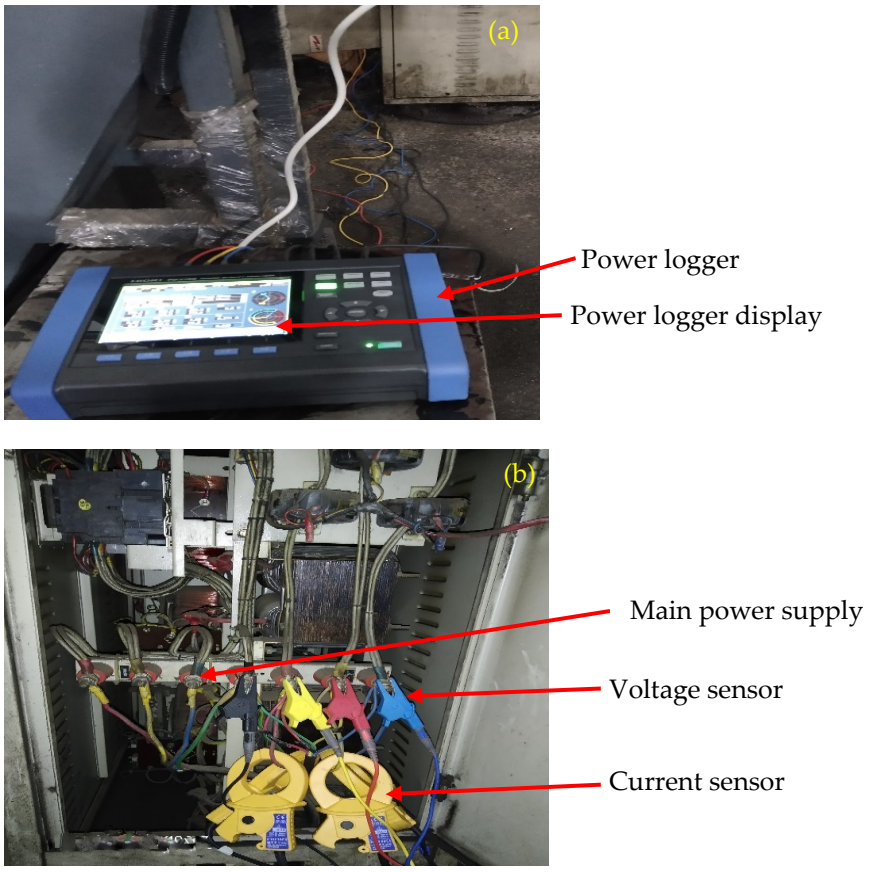

Figure 3. (**a**) Hioki power quality analyzer; (**b**) Hioki power analyzer connections.

The equipment used for making the observations was a Power Quality Analyzer, HIOKI Make, model PQ3100 (HIOKI EE Corporation, Ueda, Nagano 386-1192, Japan). The wiring mode used was 3P4W (3-Phase 4 wire). The voltage measurement was 415 V (line to line), the current sensor used was CT7126, the rated current was 60 A AC, the maximum current was 100 A peak, the maximum rated voltage to earth was 300 V AC, the anticipated transient overvoltage was 4000 V, the active power was 300 W to 9 MW with an accuracy of ±0.3% rdg. ±0.1% f.s. + clamp sensor accuracy, the measurable conductor diameter was Φ15 mm, and the measurement accuracy was as follows: frequency (45 Hz ≤ f ≤ 66 Hz), for (±0.3% rdg. ±0.1% f.s.), and phase (±0.2°).

2.1. Electric Parameters and Energy Responses

- Active power consumption by machine (ÄPC$_{m/c}$) in kW

This is the total power consumed by the machine and machining operation during the actual machining of the workpiece [41–43].

- Power factor (ƤF$_{m/c}$)

The ƤF$_{m/c}$ is the ratio of active power to apparent power, as shown in Equation (1) [36].

$$\text{ƤF}_{m/c} = \frac{\text{Active power}}{\text{Apparent power}}. \quad (1)$$

Active power is the actual power utilized to do useful work. Reactive power in (Var-volt-ampere reactive) is when the power swings back and forth without any work. It is the product of the apparent power and the sine of the phase difference (sinθ). It results from inductive loads known as lag reactive power and reactive power ensuing from ca-

pacitive loads known as lead reactive power. Apparent power in VA is obtained by combining active power and reactive power vectorially. Good ƤF usually ranges from 1.0 to 0.95, poor ƤF ranges from 0.95 to 0.85, and bad ƤF is below 0.85.

- Active energy consumption by machine (ÄEC$_{m/c}$) in kWh

This is the total energy consumed by the machine and machining operation during the actual machining of the workpiece. Energy is a product of average active power over a complete cycle, and machining time (ł$_{m/c}$) is shown in Equation (2) [36,42].

$$\text{ÄEC}_{m/c} = \text{ÄPC}_{m/c} \times \text{ł}_{m/c}. \quad (2)$$

- Energy efficiency (ĖĖ$_ή$)

This gives the ratio of the energy consumed by the machining process to the total energy consumed by the machine. The ĖĖ$_ή$ is shown in Equation (3) [36,44–47].

$$\text{ĖĖ}_ή = \frac{\text{ÄEC}_{m/c} - \text{ÄEC}_{m/c}(\text{AC})}{\text{ÄEC}_{m/c}} \times 100, \quad (3)$$

where ÄEC$_{m/c}$(AC) is the energy consumed by the machine during air cutting.

- Specific energy consumption (ş) in kJ/cm^3

This is the energy required to remove a unit volume of the material. It is obtained by dividing the total energy consumed by a machine during the machining of a workpiece by the total volume of material removed, as shown in Equation (4) [48–50].

$$\text{Specific energy consumption (ş)} = \frac{\text{ÄEC}_{m/c}}{\text{Unit volume}}. \quad (4)$$

- Current RMS (root mean square) value (Ïm/c) in ampere

The power quality analyzer records the current at an interval of 1 s. The current registered is the average of the root mean square (RMS) value of current of each of the three phases at that instant. Thus, the magnitude of the current documented and used for calculations is yet again the average of all these observations over the entire machining cycle.

- Voltage RMS value (V̈$_{av}$) in volt

The power quality analyzer logs the voltage at an interval of 1 s. The voltage measured is a line-to-line voltage in a three-phase supply. The voltage noted is the average of the RMS value of voltage across each of the three phases at that instant. Thus, the magnitude of the voltage documented and used for calculations is yet again the average of all these observations over the entire machining cycle [51].

- Current unbalance (Ïub)

This is measured as a percentage of the fundamental current, as shown in Equation (5). The three-phase power system is balanced or symmetrical if the three-phase voltages and currents have the same amplitudes and same phase shifting (angular difference) at 120° to each other. If either or both of these conditions are not met, the system is unbalanced or asymmetrical [51].

$$\text{Ï}_{ub}\ (\%) = \frac{\text{Maximum deviation from Ï}_{m/c}}{\text{Ï}_{m/c}} \times 100. \quad (5)$$

- Voltage unbalance (V̈ub)

This is measured as a percentage of the fundamental voltage, as shown in Equation (6). Thus, the current unbalance factor is several times larger than the voltage unbalance factor [51].

$$\text{V̈}_{ub}\ (\%) = \frac{\text{Maximum deviation from the average voltage}}{\text{average voltage}} \times 100. \quad (6)$$

Thus, the current unbalance causes power and energy losses. International standards such as EN-50160 and IEC 1000-3-series give limits for the unbalance voltage calculated using the ratio of sequences method up to 2% for LV (low voltage) and MV (medium voltage) systems measured as 10 min values with an instantaneous maximum of 4% [51,52].

- Current total harmonic distortion factor ($Ï_{thdf}$)

Harmonics are measured in terms of the total harmonic distortion factor. This indicates the extent to which the total harmonic component is distorting the fundamental waveform. The power quality analyzer used for experimentation can measure all types of triplen harmonics. According to the general system's IEEE 519-1992 standard, the harmonic voltage limits the maximum harmonic distortion factor's to 5.0% [41,53].

- Electrical power transients

Electrical transients are brief bursts of energy that occur on power, data, or communication networks. Transients are momentary fluctuations in voltage or current that last less than a millisecond. However, for a fraction of a second, high voltages are utilized to drive large amounts of current into an electrical circuit. The cause of the power transients may be due to utility grid switching, arc welders (arc flash), equipment cycling, grounding, lightning strike, and voltage/current drops [41,53].

2.2. Experimental Procedure, Observations, and Calculations

Under the current study, a particular industry was selected. Five separate machining operations on different machine tools were considered. These operations were designated as O-1 to O-5. Details of these machining operations were presented in Section 2.1. The machine tools were placed in the machine shop of the industry. The experiment was performed under the actual operating conditions. Other machine tools in the vicinity of the machine tool under study were simultaneously functioning. Power and electric parameters for each of the machining operations were noted with the help of the Hioki-3100 power quality analyzer attached to the main power supply of the machine tool. Readings were noted at an interval of 1 s. The data obtained were analyzed with the help of Hioki PQ-one version 4.00 software (HIOKI EE Corporation, Ueda, Nagano 386-1192, Japan. The machining time for each operation was carefully noted. Three sets of observations were recorded for each of the machining operations.

Furthermore, two types of observations were made for each machining operation, first under air cutting (AC) and then under an actual cut. In air cutting, observations were recorded without actual cutting taking place, whereas, under the actual cut, observations were recorded when actual cutting or machining was taking place.

The observations were stored in the SD memory card of the power quality analyzer. The memory card was then transferred to the laptop or computer where the Hioki PQ-1 software Ver. 4.00 was installed, and different electric parameters were recorded at an interval of 1 s for the entire duration of the machining operation. The observed data were tabulated under an excel chart. The average values of each electric parameter corresponding to each machining operation were noted. In the study, the machining processes did not have any power transients due to switching, welding, equipment cycling, grounding, and lightning supplies. Consequently, these were not taken into account as factors affecting electric parameters. Furthermore, motor conditions for machines such as VMC/CNC do not change perceptibly with time and remain for a long time. Moreover, the machine tools under study were no more than 3 years old; thus, this effect was negligible. Higher-order harmonics (e.g., fifth and ninth) were seen in the observations, but their percentage values were too minimal to make an impact; hence, they could be safely rejected. Moreover, these harmonics were well within IEEE 519 and even EN50160 harmonic ratings or permissible limits. The experimental observations and calculations for air cutting, i.e., without machining, are shown in Table 5.

Table 5. Experimental observations and calculations of air cutting (without machining).

Operation	ℓm/c	ÄPCAC	ÄECAC	Ïm/c	Ïthdf	Ïub	V̈av	V̈ub	V̈thdf
O-1	154	1.467	0.062	3.335	26.345	33.645	416.540	2.658	3.132
O-2	104	1.449	0.041	3.277	26.676	31.750	411.223	1.570	5.406
O-3	76	2.205	0.046	5.423	29.082	14.240	415.302	0.410	2.149
O-4	77	1.080	0.023	2.457	41.035	35.515	417.354	0.260	2.255
O-5	63	1.626	0.030	3.594	52.480	12.930	428.041	0.260	5.900

Active energy consumption was calculated as per Equation (2). The experimental observations taken from the power logger for actual cutting, i.e., during machining operations for operations O-1 to O-5, are shown in Table 6. The calculations of active energy, energy efficiency, and specific energy consumption as per Equations (2), (3), and (4) are shown in Table 7. These data were used to evaluate the impact of electric parameters on active power consumption and ascertain a methodology to identify and prioritize the most energy-intensive machining processes.

Table 6. Experimental observations of the actual cut (machining).

Operation	ℓm/c (sec)	ÄPCm/c (kW)	ÄECm/c (kWh)	V (cm³)	ÞFm/c	Ïm/c (A)	Ïthdf (%)	Ïub (%)	V̈av (V)	V̈ub (%)	V̈thdf (%)
O-1	154	1.973	0.084	19.759	0.677	4.027	40.898	40.316	415.500	2.58	3.638
O-2	104	2.321	0.067	19.759	0.675	4.719	40.965	35.670	409.706	1.630	6.565
O-3	76	3.706	0.077	19.702	0.686	7.404	41.435	10.94	415.234	0.405	2.26
O-4	77	1.542	0.033	3.760	0.647	3.478	43.673	18.583	416.825	0.225	2.257
O-5	63	2.975	0.053	14.300	0.738	5.691	51.447	19.420	426.704	0.285	6.349

Table 7. Calculations of actual cut during O-1 to O-5.

Operation	ÄECm/c (kJ)	ĖĖή (%)	ş (kJ/cm³)
O-1	302.472	25.637	15.308
O-2	241.200	38.209	12.207
O-3	277.74	40.260	14.097
O-4	118.620	30.303	31.548
O-5	190.800	43.396	13.343

3. Regression Models of Active Power Consumption for Machining Operations

This section describes the multiple regression modeling of active power consumption in each machining operation from O-1 to O-5. Experiments were carried out in the real world at a machine shop in the industry. They were not carried out in a laboratory under controlled settings. Many machine tools and pieces of equipment were used simultaneously, along with the observed machine tools. As a result, the quality of the electric power supplied to the machine tool was affected. Therefore, the main aim of the regression modeling was to identify the significant electric parameters affecting the active power consumed by the machining operations. The predictors or the independent variables considered were the following electric parameters: the average current, power factor, current total harmonic distortion factor, current unbalance, voltage unbalance, average voltage, and voltage total harmonic distortion factor.

The regression models for the five machining operations were developed using the backward elimination method. This involved eliminating nonsignificant terms from the model. The elimination of nonsignificant terms is based on the *p*-value of the *t*-statistic test evaluated at $\alpha = 0.05$ for each of the predictors. If the *p*-value was higher than 0.05, the predictor was considered nonsignificant. The coefficient of determination (R^2) and

ANOVA were used to assess the fitness of the proposed model. The R-squared value describes the variance in the response data interpreted by the regression model. The model's predicted R-squared (pred) indicates how it might anticipate data. When unnecessary variables are included in the model, the adjusted R-squared (adj) will typically decrease. There is a good chance that significant terms have been introduced into the model if the difference between R-squared and R-squared (adj) is small [54].

The regression models were made with coded regression coefficients. These were obtained by subtracting the mean from each predictor's value and dividing it by the standard deviation. Coded coefficients help to determine the relative importance of each of the significant predictors to the dependent variable. The R-squared Value was noted after the first iteration of the regression modeling process. The R-squared values are shown in Table 8.

Table 8. Coefficient of determination (R-sq.) for O-1 to O-5.

Operation	Iteration-1		Final Iteration	
	R-Sq.	(%)	Non-Significant Terms Removed	R-Sq. (%)
O-1	R-sq.	98.56	$\dot{V}_{ub}$, $\dot{V}_{thdf}$, $\dot{I}_{ub}$	98.55
	R-sq. (adj)	98.50		98.51
	R-sq. (pred)	98.19		98.27
O-2	R-sq.	99.52	$\dot{V}_{ub}$, $\dot{V}_{thdf}$, $\dot{I}_{thdf}$	99.50
	R-sq. (adj)	99.48		99.48
	R-sq. (pred)	99.39		99.42
O-3	R-sq.	99.69	$\dot{V}_{thdf}$, $\dot{I}_{thdf}$, $\dot{V}_{av}$, $\dot{I}_{ub}$	99.65
	R-sq. (adj)	99.66		99.64
	R-sq. (pred)	99.46		99.49
O-4	R-sq.	98.60	$\dot{V}_{ub}$, $\dot{V}_{av}$, $\dot{I}_{ub}$	98.41
	R-sq. (adj)	98.46		98.33
	R-sq. (pred)	98.07		98.02
O-5	R-sq.	93.96	$\dot{V}_{thdf}$, $\dot{V}_{av}$	93.64
	R-sq. (adj)	93.20		93.08
	R-sq. (pred)	89.57		89.30

The developed regression equations for machining operations in uncoded regression coefficients from O-1 to O-5 are shown in Equation (7) to Equation (11).

$$\text{ÄPC}_{m/c}\text{ (O-1)} = -12{,}133 + 23.8\ \dot{V}_{av} + 7.893\ \dot{I}_{thdf} + 3964.8\ \text{PF}_{m/c} + 301.4\ \dot{I}_{m/c}. \quad (7)$$

$$\text{ÄPC}_{m/c}\text{ (O-2)} = -17{,}763 + 13.25\ \dot{I}_{ub} + 34.97\ \dot{V}_{av} + 4494\ \text{PF}_{m/c} + 478.76\ \dot{I}_{m/c}. \quad (8)$$

$$\text{ÄPC}_{m/c}\text{ (O-3)} = -1621 - 1441\ \dot{V}_{ub} + 2316\ \text{PF}_{m/c} + 582.94\ \dot{I}_{m/c}. \quad (9)$$

$$\text{ÄPC}_{m/c}\text{ (O-4)} = -1618 - 418\ \dot{V}_{thdf} + 6.466\ \dot{I}_{thdf} + 4002\ \text{PF}_{m/c} + 355.57\ \dot{I}_{m/c}. \quad (10)$$

$$\text{ÄPC}_{m/c}\text{ (O-5)} = -5019 - 11296\ \dot{V}_{ub} + 68.4\ \dot{I}_{ub} + 24.7\ \dot{I}_{thdf} + 6853\ \text{PF}_{m/c} + 629.2\ \dot{I}_{m/c}. \quad (11)$$

After removing nonsignificant terms (p-values greater than 0.05), final models of active power for each operation were accepted with electric parameters having significant effects (p-value less than 0.05). The results of ANOVA are shown in Table 9. The coded coefficients for machining operations from O-1 to O-5 are shown in Table 10.

Table 9. ANOVA Table for O-1 to O-5.

Source	DF	Adj SS	Adj MS	F-Value	*p*-Value
		O-1			
Regression	4	41,924,033	10,481,008	2526.98	0.000
Error	149	617,999	4148		
Total	153	42,542,032			
		O-2			
Regression	4	103,689,348	25,922,337	4895.57	0.000
Error	99	524,211	5295		
Total	103	104,213,559			
		O-3			
Regression	3	68,657,447	22,885,816	6859.26	0.000
Error	72	240,227	3336		
Total	75	68,897,674			
		O-4			
Regression	4	19,636,536	4,909,134	1117.05	0.000
Error	72	316,419	4395		
Total	76	19,952,955			
		O-5			
Regression	5	143,722,619	28,744,524	167.81	0.000
Error	57	9,763,666	171,292		
Total	62	153,486,286			

Table 10. Coded regression coefficients for O-1 to O-5.

Term	Coef	SE Coef	T-Value	*p*-Value	VIF
		O-1			
Constant	1942.20	5.19	374.24	0.000	
V̈av	12.04	5.39	2.23	0.000	1.07
Ïthdf	82.22	8.76	9.39	0.000	2.83
ƤF$_{m/c}$	369.48	7.55	48.93	0.000	2.10
Ï$_{m/c}$	239.48	8.97	26.71	0.000	2.95
		O-2			
Constant	2302.78	7.14	322.73	0.000	
Ï$_{ub}$	96.0	11.7	8.19	0.000	2.67
V̈$_{av}$	30.05	8.04	3.74	0.000	1.26
ƤF$_{m/c}$	386.7	13.8	28.03	0.000	3.70
Ï$_{m/c}$	755.8	10.8	69.77	0.000	2.28
		O-3			
Constant	3685.24	6.63	556.20	0.000	
V̈$_{ub}$	−30.80	6.91	-4.46	0.000	1.07
ƤF$_{m/c}$	158.1	13.2	11.94	0.000	3.94
Ï$_{m/c}$	816.1	13.1	62.42	0.000	3.84
		O-4			
Constant	1528.34	7.55	202.30	0.000	
V̈$_{thdf}$	−17.43	8.09	−2.15	0.035	1.13

Ïthdf	105.1	13.8	7.60	0.000	3.30
ƤFm/c	431.4	13.0	33.31	0.000	2.90
Ïm/c	415.02	8.96	46.34	0.000	1.39
		O-5			
Constant	2942.9	52.1	56.44	0.000	
V̈ub	−183.9	62.2	−2.96	0.005	1.40
Ïub	367	180	2.04	0.046	11.68
Ïthdf	218.9	98.9	2.21	0.031	3.54
ƤFm/c	1108.4	61.2	18.12	0.000	1.35
Ïm/c	1211	133	9.11	0.000	6.40

3.1. Analysis of the Regression Model for Operation-1 (O-1)

In machining operation O-1, the overall regression model as per Equation (7) was statistically the best fit because the coefficient of determination as per Table 8 after the final iteration had values of R-sq. 98.50% and R-sq. (adj) 98.47%. This means that the regression model explained the maximum variation of the dependent variable, which was active power, up to 98.47%. A look at the residual plots for ÄPCm/c for (O-1) in Figure 4b indicates that the residuals lie close to the diagonal line representing an ideal normal distribution. The points of the residual plots were not skewed, and they were randomly distributed. Therefore, it seems that the data were normally distributed. Furthermore, a look at the histogram of residuals gives evidence that our residuals were normally distributed. The distribution of residuals along the straight horizontal line was similar for all significant parameters, suggesting equality of variance. Therefore, the conditions of normality of residuals and equality of variance were fulfilled. The ANOVA results for (O-1) revealed that there was significance between-group variance according to the value of the F-statistic (see Table 9). At $\alpha = 0.05$, the F-value was equal to 2526.98 with a p-value < 0.001. This indicates evidence of a regression relationship between the dependent variable ÄPCm/c and the independent variables ƤFm/c, Ïm/c, V̈av, and Ïthdf combined.

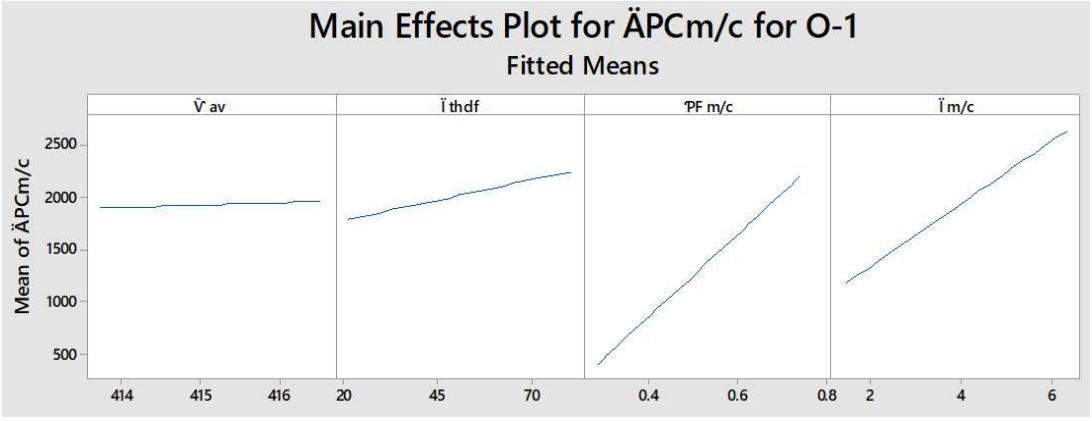

(**a**)

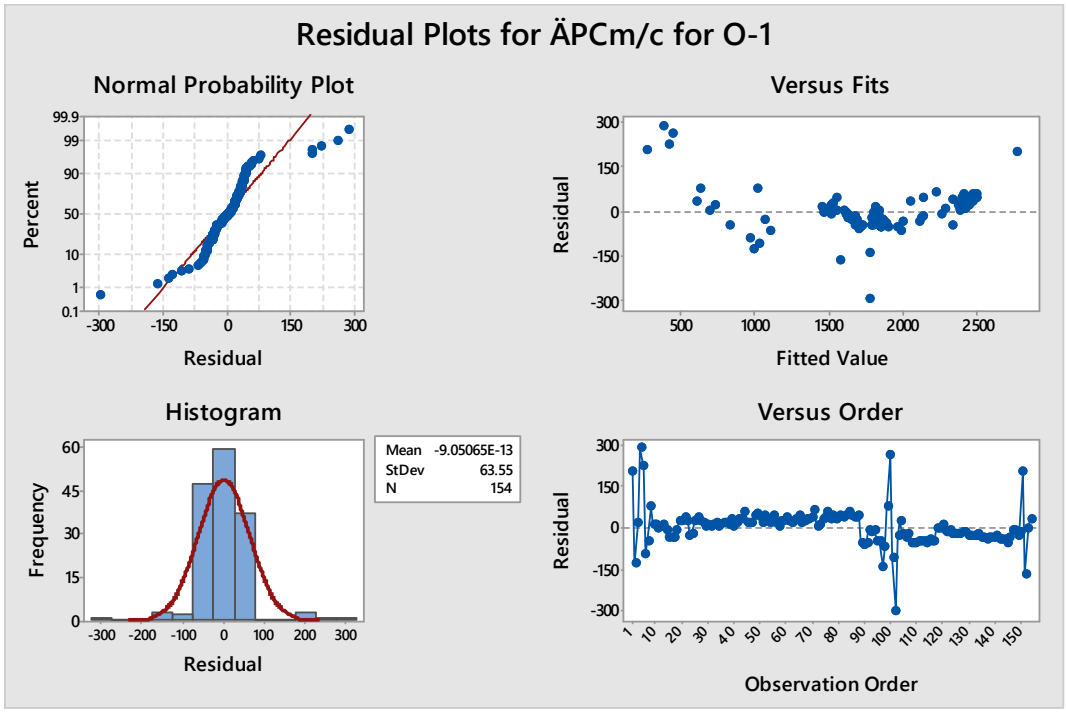

(**b**)

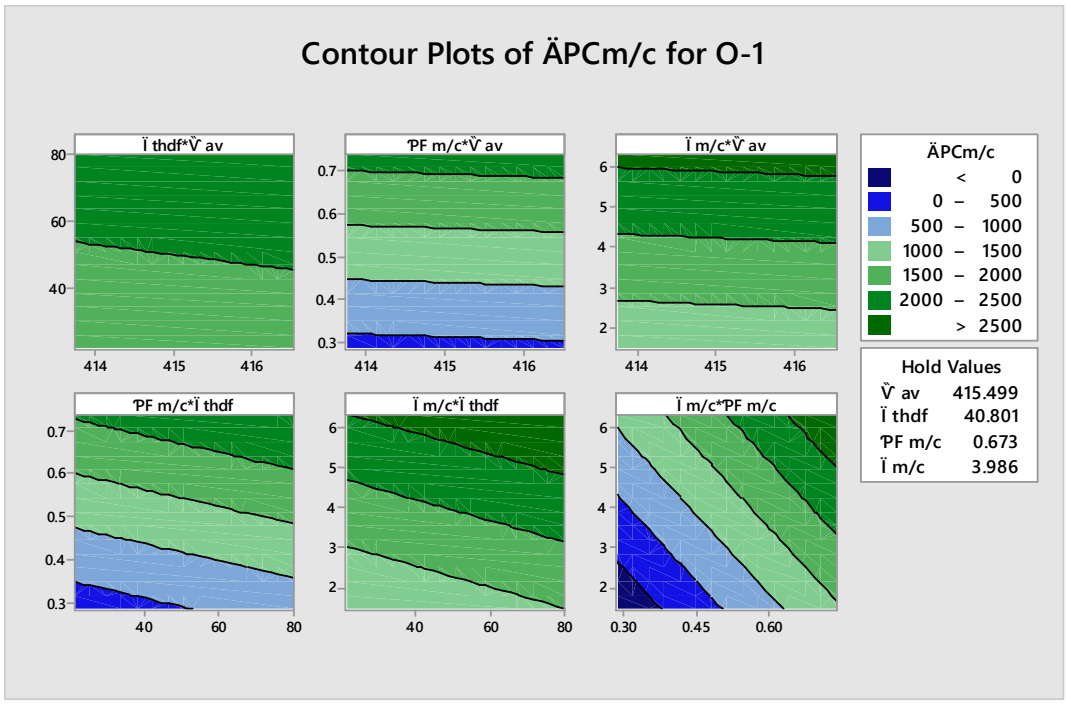

(**c**)

Figure 4. (**a**) Main effects plot for O-1. (**b**) Residuals plot for O-1. (**c**) Contour plots for O-1.

Individual coefficients contributed meaningful information in the prediction of $ÄPC_{m/c}$ (see Table 10 for O-1). The test statistics showed significant *t*-values of $Ṕ F_{m/c}$, $Ï_{m/c}$, $V̈_{av}$, and $Ï_{thdf}$ at $\alpha = 0.05$. Therefore, $Ṕ F_{m/c}$, $Ï_{m/c}$, $V̈_{av}$, and $Ï_{thdf}$ were individually useful in the prediction of $ÄPC_{m/c}$. The coded coefficients in Table 10 reveal that, for machining operation O-1, the predictor with the highest impact on the dependent variable $ÄPC_{m/c}$ was $Ṕ F_{m/c}$

(369.48), followed by $Ï_{m/c}$ (239.48), $Ï_{thdf}$ (82.22), and $Ṽ_{av}$ (12.04). The value of the VIF (variance inflation factor) in Table 10 for O-1 of all predictors was less than 5. This indicates that there was no significant multicollinearity between the significant predictors.

A look at the main effects plots for $ÄPC_{m/c}$ in Figure 4a also validates the above result. The slope of significant predictors versus $ÄPC_{m/c}$ indicates that, in this machining operation (O-1), $ƤF_{m/c}$ had a maximum impact on $ÄPC_{m/c}$, followed by $Ï_{m/c}$, $Ï_{thdf}$, and $Ṽ_{av}$.

The contour plots of $Ï_{m/c}$, $ƤF_{m/c}$, and $ÄPC_{m/c}$ in Figure 4c indicate the maximum impact of $Ï_{m/c}$ and $ƤF_{m/c}$ on $ÄPC_{m/c}$ as the number of contour lines representing different ranges of $ÄPC_{m/c}$ consumption was greater. This suggests that any variation in $Ï_{m/c}$ and $ƤF_{m/c}$ significantly affects the power consumption. The contour plot between $ƤF_{m/c}$ and $Ï_{thdf}$ and between $Ï_{m/c}$ and $Ï_{thdf}$ indicate that both parameters were significant, but their impact on $ÄPC_{m/c}$ was not as substantial as $Ï_{m/c}$ and $ƤF_{m/c}$, whereas the plot between $Ï_{thdf}$ and $Ṽ_{av}$ exhibited the least significance.

3.2. Analysis of the Regression Model for Operation-2 (O-2)

In the machining operation O-2, the overall regression model as per Equation (8) was statistically the best fit because the coefficient of the determination as per Table 8 after the final iteration had values of R-sq. 99.50% and R-sq. (adj) 99.48%. This means that the regression model explained the maximum variation of the active power up to 99.48%. A look at the residual plots for $ÄPC_{m/c}$ for (O-2) in Figure 5b indicates that the residuals lie close to the diagonal line, representing an ideal normal distribution. The points of the residual plots were not skewed, and they were randomly distributed. Therefore, it seems that the data were normally distributed. Furthermore, a look at the histogram of residuals gives evidence that our residuals were normally distributed. The distribution of residuals along the straight horizontal line was similar for all significant parameters, suggesting equality of variance. Therefore, the conditions of normality of residuals and equality of variance were fulfilled. The ANOVA results for O-2 revealed that there was significant between-group variance based on the value of the F-statistic (see Table 9). At $\alpha = 0.05$, the F-value was equal to 4895.57 (p-value < 0.001). This indicates evidence of a regression relationship between the dependent variable $ÄPC_{m/c}$ and the independent variables $ƤF_{m/c}$, $Ï_{m/c}$, $Ṽ_{av}$, and $Ï_{ub}$ combined.

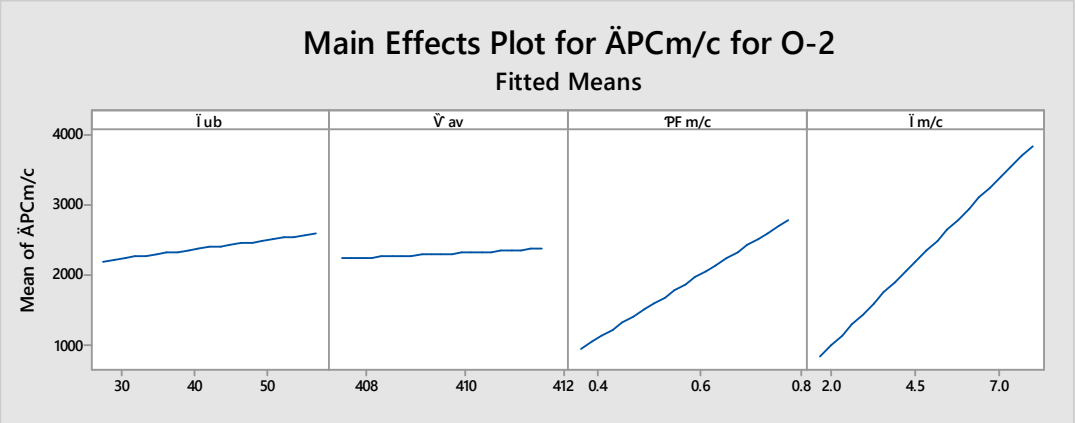

(**a**)

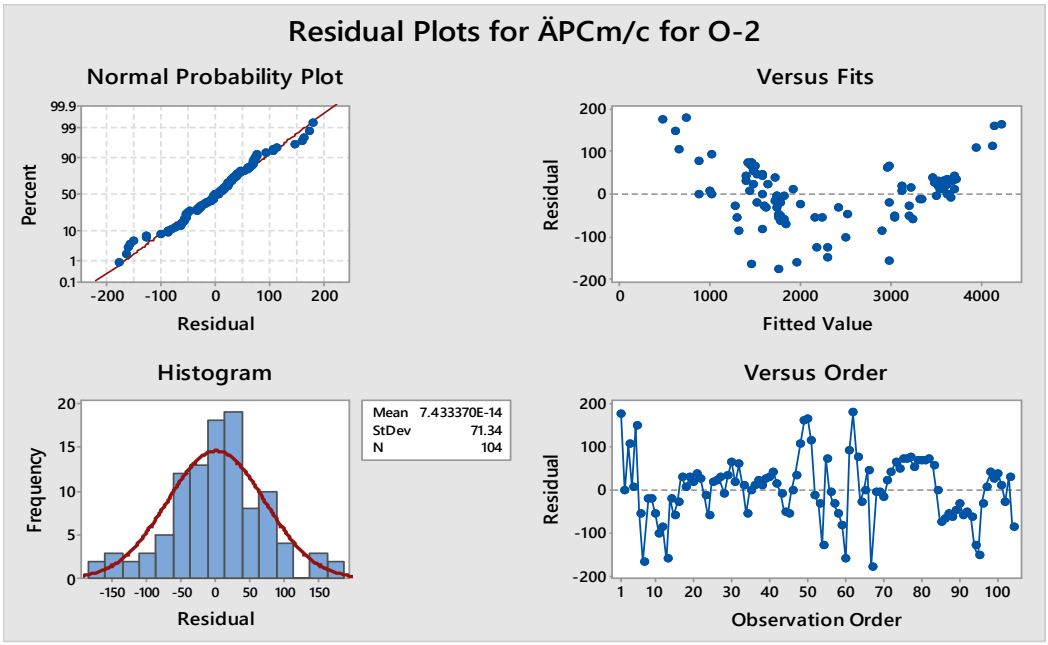

(**b**)

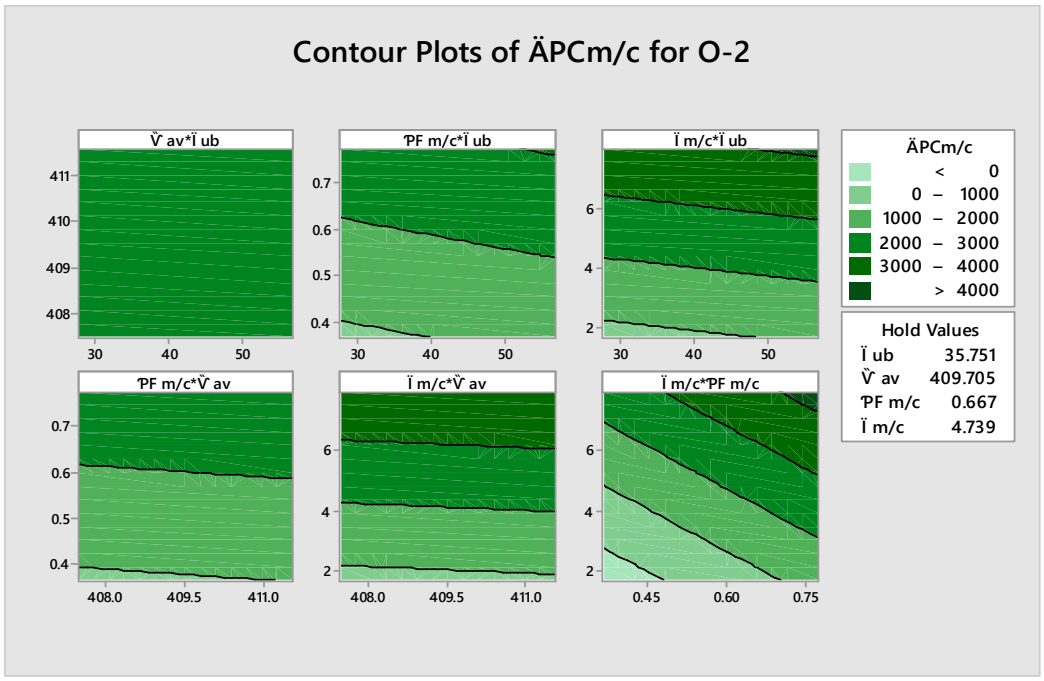

(**c**)

Figure 5. (**a**) Main effects plot for O-2. (**b**) Residuals plot for O-2. (**c**) Contour plots for O-2.

Individual coefficients contributed meaningful information to the prediction of $ÄPC_{m/c}$ (see Table 10 for O-2). The test statistics showed *t*-values of $Ƥ F_{m/c}$, $Ï_{m/c}$, $V̈_{av}$, and $Ï_{ub}$ at $\alpha = 0.05$. Therefore, $Ƥ F_{m/c}$, $Ï_{m/c}$, $V̈_{av}$, and $Ï_{ub}$ were individually useful in the prediction of $ÄPC_{m/c}$. The coded coefficients in Table 10 reveal that, for machining operation O-2, the predictor with the highest impact on the dependent variable $ÄPC_{m/c}$ was $Ï_{m/c}$ (755.8) followed by $Ƥ F_{m/c}$ (386.7), $Ï_{ub}$ (96.0), and $V̈_{av}$ (30.05). The value of the VIF (variance inflation factor) in Table 10 for O-2 of all predictors was less than 5. This indicates that there was no significant multicollinearity between the significant predictors.

A look at the main effects plots for ÄPC$_{m/c}$ in Figure 5a also validates the above result. The slope of significant predictors versus ÄPC$_{m/c}$ indicates that, in this machining operation (O-2), Ï$_{m/c}$ had the maximum impact on ÄPC$_{m/c}$, followed by, ƤF$_{m/c,}$ Ï$_{ub}$, and V̈$_{av}$.

The contour plots of Ï$_{m/c}$, ƤF$_{m/c,}$ and ÄPC$_{m/c}$ in Figure 5c indicate the maximum impact of Ïm/c and ƤF$_{m/c}$ on ÄPC$_{m/c}$ as the number of contour lines representing different ranges of ÄPC$_{m/c}$ consumption was greater. This suggests that any variation in Ï$_{m/c}$ and ƤF$_{m/c}$ significantly affected the power consumption. The contour plots between ƤF$_{m/c}$ and Ï$_{ub}$ and between Ï$_{m/c}$ and Ï$_{ub}$ indicate that both parameters were significant, but their impact on ÄPC$_{m/c}$ was not as substantial as Ï$_{m/c}$ and ƤF$_{m/c}$, whereas the plot between Ï$_{ub}$ and V̈$_{av}$ exhibited the least significance.

3.3. Analysis of the Regression Model for Operation-3 (O-3)

In the machining operation O-3, the overall regression model as per Equation (9) was statistically the best fit because the coefficient of determination as per Table 8 after the final iteration had values of R-sq. 99.65% and R-sq. (adj) 99.64%. This means that the regression model explained the maximum variation of the active power up to 99.64%. A look at the residual plots for ÄPC$_{m/c}$ for (O-3) in Figure 6b indicates that the residuals lie close to the diagonal line representing an ideal normal distribution. The points of the residual plots were not skewed, and they were randomly distributed. Therefore, it seems that the data were normally distributed. Furthermore, a look at the histogram of residuals gives evidence that our residuals were normally distributed. The distribution of residuals along the straight horizontal line was similar for all significant parameters, suggesting equality of variance. Therefore, the conditions of normality of residuals and equality of variance were fulfilled. The ANOVA results for O-3 revealed that there was significant between-group variance based on the value of the F-statistic (see Table 9). At $\alpha = 0.05$, the F-value was equal to 6859.26 with a p-value < 0.001. This indicates evidence of a regression relationship between the dependent variable ÄPC$_{m/c}$ and the independent variables ƤF$_{m/c}$, Ï$_{m/c}$, and V̈$_{ub}$ combined.

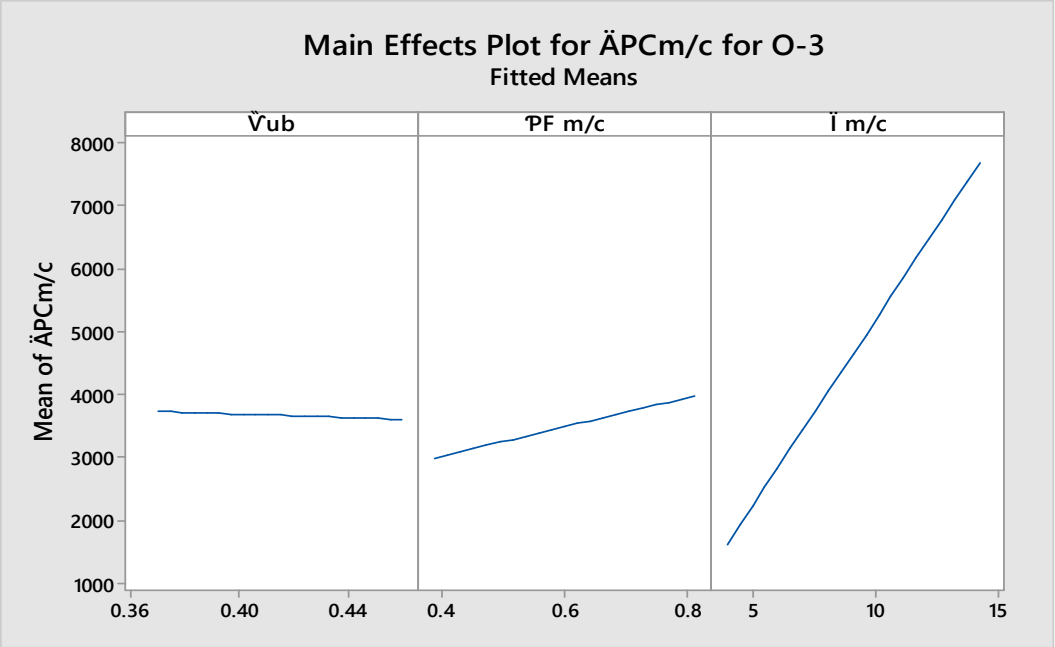

(**a**)

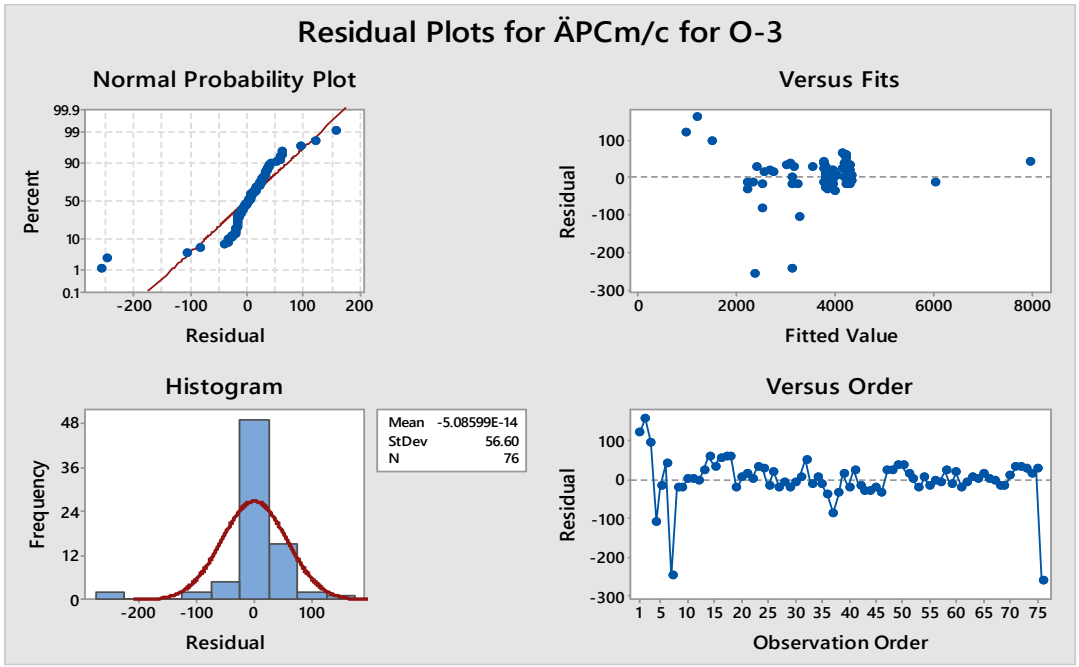

(**b**)

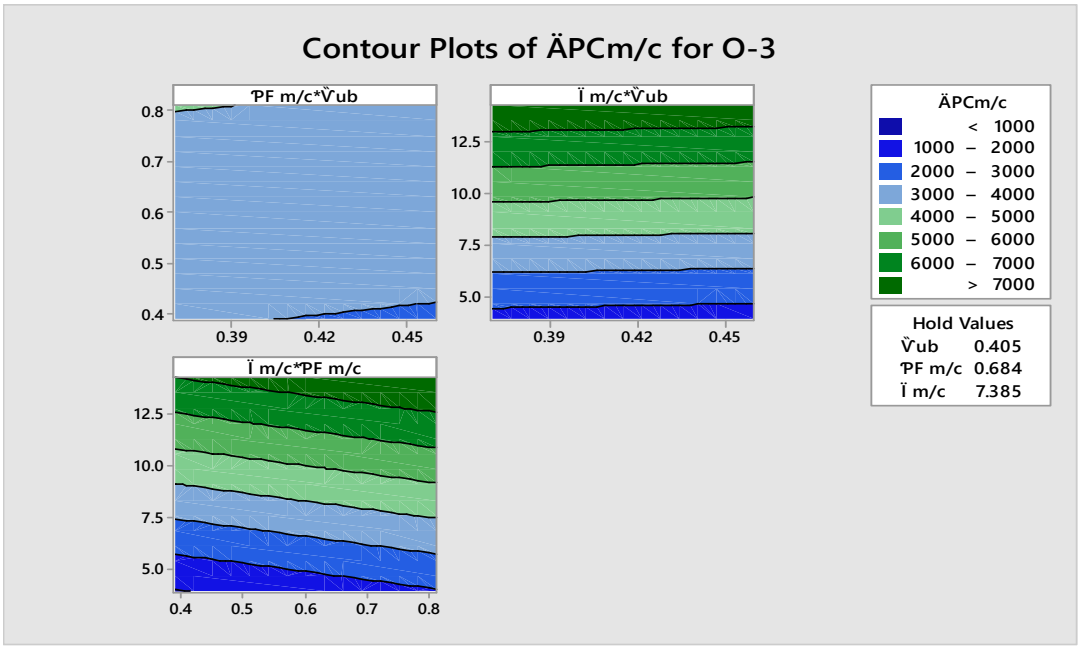

(**c**)

Figure 6. (**a**) Main effects plot for O-3. (**b**) Residuals plot for O-3. (**c**) Contour plots for O-3.

Individual coefficients contributed meaningful information in the prediction of $ÄPC_{m/c}$ (see Table 10 for O-3). The test statistics showed *t*-values of $ƤF_{m/c}$, $Ï_{m/c}$, and $V̌_{ub}$ at $\alpha = 0.05$. Therefore, $ƤF_{m/c}$, $Ï_{m/c}$, and $V̌_{ub}$ were individually useful in the prediction of $ÄPC_{m/c}$. The coded coefficients in Table 10 reveal that, for machining operation O-3, the predictor with the highest impact on the dependent variable $ÄPC_{m/c}$ was $Ï_{m/c}$ (816.1), followed by $ƤF_{m/c}$ (158.1) and $V̌_{ub}$ (−30.80). The negative sign indicates that the predictor $V̌_{ub}$ had the highest negative effect on the consumption of $ÄPC_{m/c}$. The value of the VIF (variance inflation factor) inTable 10 for O-3 of all predictors was less than 5. This indicates that there was no significant multicollinearity between the significant predictors.

A look at the main effects plots for ÄPC$_{m/c}$ in Figure 6a also validates the above result. The slope of significant predictors versus ÄPC$_{m/c}$ indicates that, in this machining operation (O-3), Ï$_{m/c}$ had the maximum impact on ÄPC$_{m/c}$, followed by ƤF$_{m/c}$, whereas V̈$_{ub}$ had a negative slope.

The contour plots of Ï$_{m/c}$, ƤF$_{m/c,}$ and ÄPC$_{m/c}$ in Figure 6c indicate the maximum impact of Ïm/c and ƤF$_{m/c}$ on ÄPC$_{m/c}$ as the number of contour lines representing different ranges of ÄPC$_{m/c}$ consumption was greater. This suggests that any variation in Ï$_{m/c}$ and ƤF$_{m/c}$ significantly affected the power consumption. The contour plot between Ï$_{m/c}$ and V̈$_{ub}$ indicates that both parameters were significant, but their impact on ÄPC$_{m/c}$ was not as substantial as Ï$_{m/c}$ and ƤF$_{m/c}$, whereas the plot between ƤF$_{m/c}$ and V̈$_{ub}$ exhibited the least significance.

3.4. Analysis of the Regression Model for Operation-4 (O-4)

In the machining operation O-4, the overall regression model as per Equation (10) was statistically the best fit because the coefficient of determination as per Table 8 for O-4, after the final iteration, had values of R-sq. 98.41% and R-sq. (adj) 98.33%. This means that, for O-4, the regression model explained the maximum variation of the active power up to 98.33%. A look at the residual plots for ÄPC$_{m/c}$ for (O-4) in Figure 7b indicates that the residuals lie close to the diagonal line, representing an ideal normal distribution. The points of the residual plots were not skewed, and they were randomly distributed. Therefore, it seems that the data were normally distributed. Furthermore, a look at the histogram of residuals gives evidence that our residuals were normally distributed. The distribution of residuals along the straight horizontal line was similar for all significant factors, suggesting equality of variance. Therefore, the conditions of normality of residuals and equality of variance were fulfilled. The ANOVA results for O-4 revealed that there was significant between-group variance based on the value of the F-statistic (see Table 9). At $\alpha = 0.05$, the F-value was equal to 1117.05 (p-value < 0.001). This indicates evidence of a regression relationship between the dependent variable ÄPC$_{m/c}$ and the independent variables ƤF$_{m/c}$, Ï$_{m/c}$, Ï$_{thdf}$, and V̈$_{thdf}$ combined.

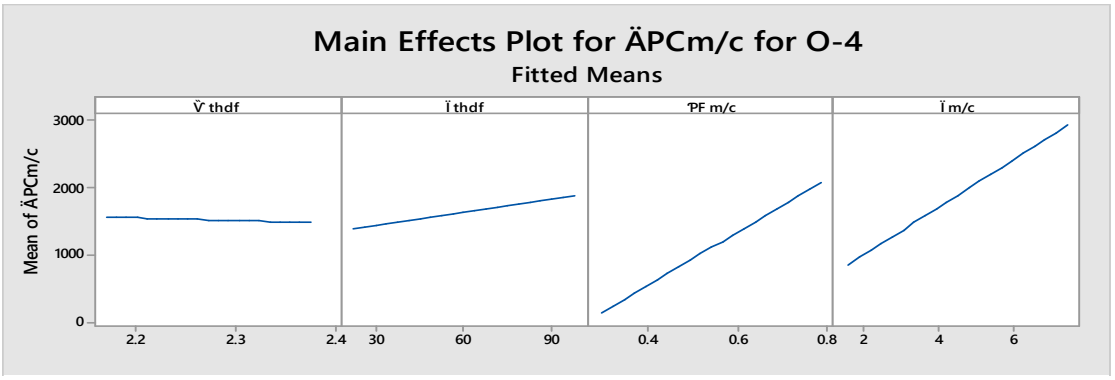

(**a**)

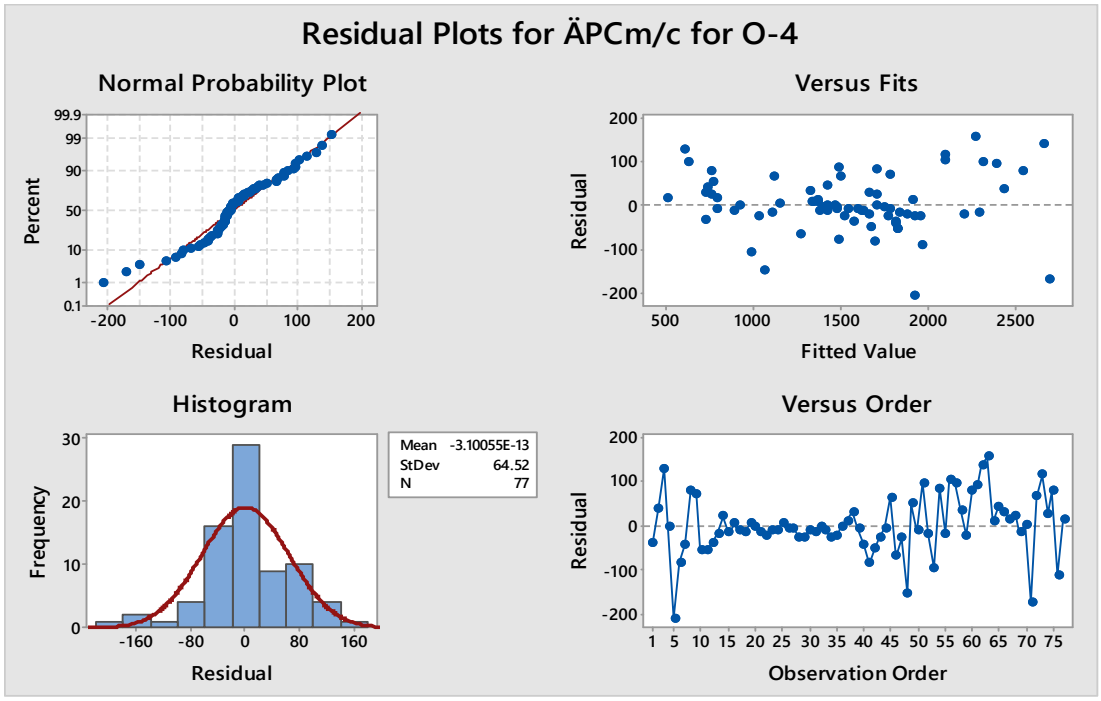

(**b**)

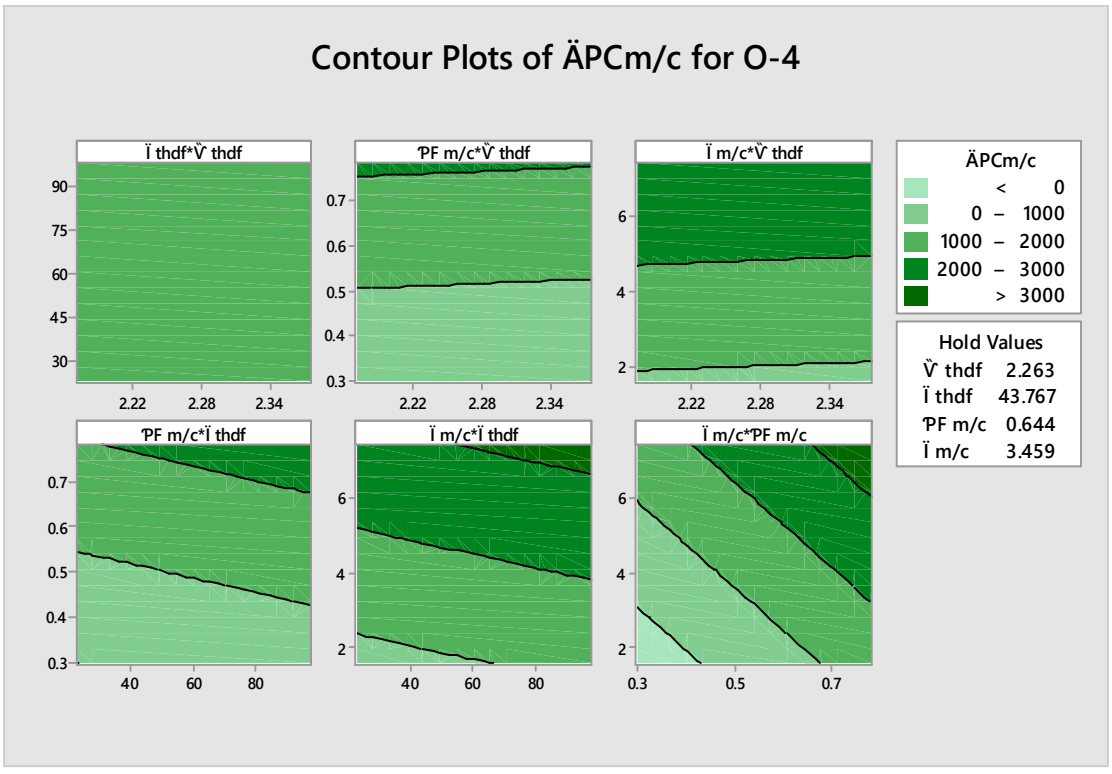

(**c**)

Figure 7. (**a**) Main effects plot for O-4. (**b**) Residuals plot for O-4. (**c**) Contour plots for O-4.

Individual coefficients contributed meaningful information in the prediction of $ÄPC_{m/c}$ (see Table 10 for O-4). The test statistics showed *t*-values of $ƤF_{m/c}$, $Ï_{m/c}$, $Ï_{thdf,}$ and $V̈_{thdf}$ at $\alpha = 0.05$. Therefore, $ƤF_{m/c}$, $Ï_{m/c}$, $Ï_{thdf}$, and $V̈_{thdf}$ were individually useful in the prediction of $ÄPC_{m/c}$. The coded coefficients in Table 10 reveal that, for machining operation O-4, the predictor with the highest impact on the dependent variable $ÄPC_{m/c}$ was $ƤF_{m/c}$ (431.4), followed by $Ï_{m/c}$ (415.02), $Ï_{thdf}$ (105.1), and $V̈_{thdf}$ (−17.43). The negative sign indicates that the

predictor V̈ub had the highest negative effect on the consumption of ÄPCm/c. The value of the VIF (variance inflation factor) in Table 10 for O-4 of all predictors was less than 5. This indicates that there was no significant multicollinearity between the significant predictors. A look at the main effects plots for ÄPCm/c in Figure 7a also validates the above result. The slope of significant predictors versus ÄPCm/c indicates that, in this machining operation (O-4), ƤFm/c had the maximum impact on ÄPCm/c, followed by Ïm/c, and Ïthdf. The plots also show that V̈thdf had a slight negative slope.

For O-4, the contour plots of Ïm/c, ƤFm/c, and ÄPCm/c in Figure 7c indicate the maximum impact of Ïm/c and ƤFm/c on ÄPCm/c as the number of contour lines representing different ranges of ÄPCm/c consumption was greater. This suggests that any variation in Ïm/c and ƤFm/c significantly affected the power consumption. The contour plot between Ïm/c and Ïthdf indicates that both parameters were significant, but their impact on ÄPCm/c was not as substantial as Ïm/c and ƤFm/c. The impact of Ïthdf and V̈thdf on ÄPCm/c was the least significant.

3.5. Analysis of the Regression Model for Operation-5 (O-5)

In the machining operation O-5, the overall regression model as per Equation (11) was statistically the best fit because the coefficient of the determination as per Table 8 for O-5, after the final iteration, had values of R-sq. 93.64% and R-sq. (adj) 93.08%. This means that, for O-5, the regression model explained the maximum variation of the active power up to 93.08%. A look at the residual plots for ÄPCm/c for (O-5) in Figure 8b indicates that the residuals lie close to the diagonal line, representing an ideal normal distribution. The points of the residual plots were not skewed, and they were randomly distributed. Therefore, it seems that the data were normally distributed. Furthermore, a look at the histogram of residuals gives evidence that our residuals were normally distributed. The distribution of residuals along the straight horizontal line was similar for all significant parameters, suggesting equality of variance. Therefore, the conditions of normality of residuals and equality of variance were fulfilled.

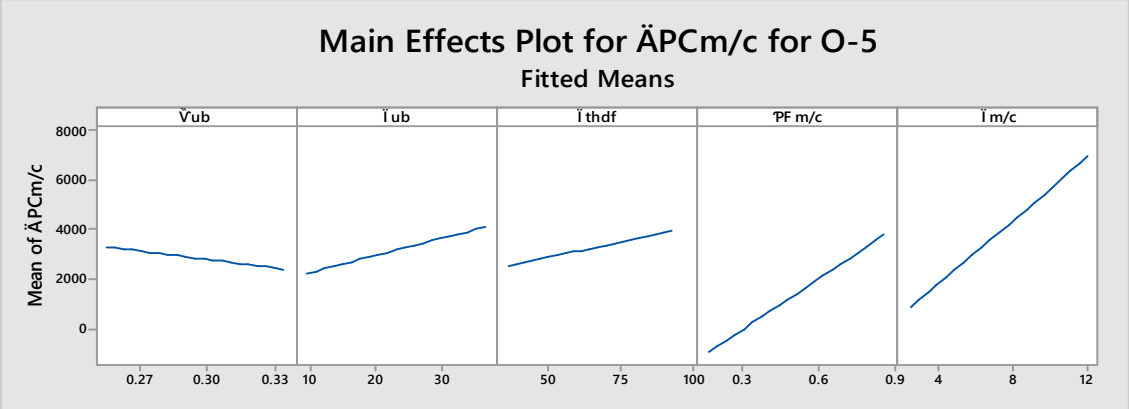

(**a**)

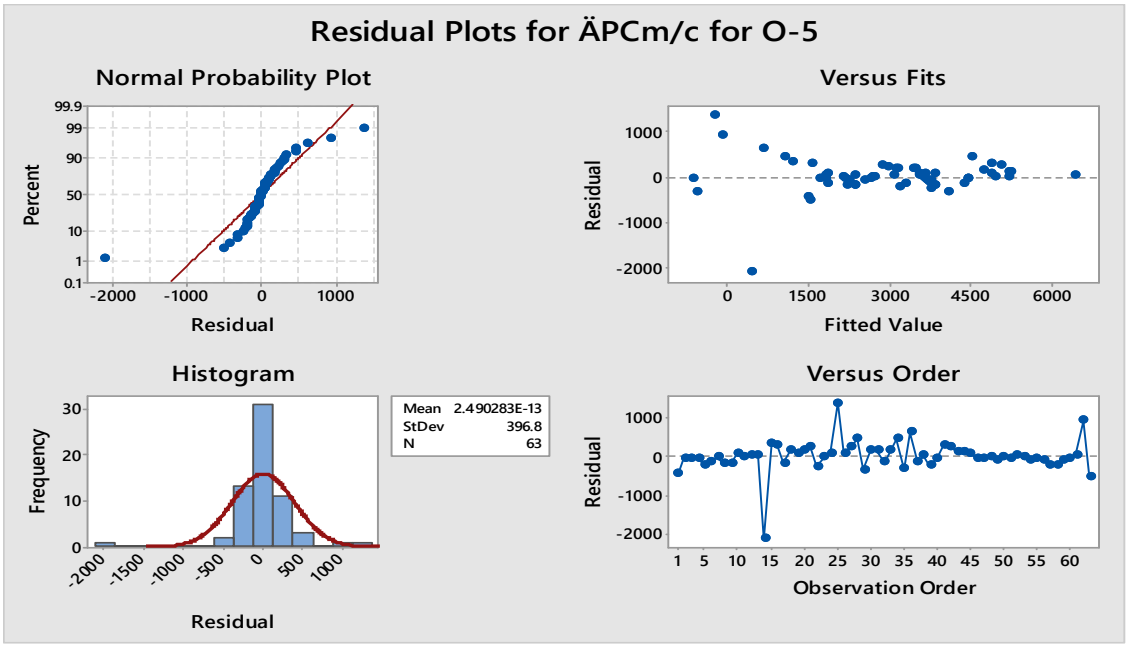

(**b**)

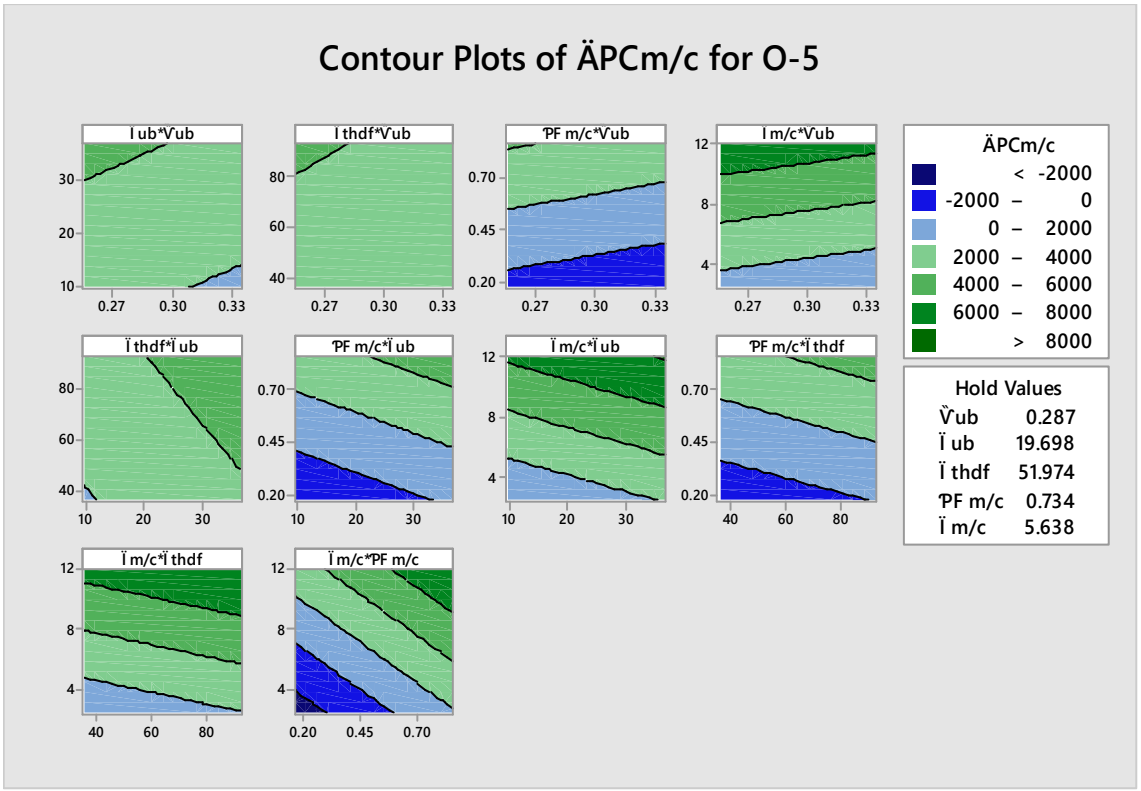

(**c**)

Figure 8. (**a**) Main effects plot for O-5. (**b**) Residuals plot for O-5. (**c**) Contour plots for O-5.

The ANOVA results for O-5 reveal that there was significant between-group variance based on the value of the F-statistic (see Table 9). At $\alpha = 0.05$, the F-value was equal to 167.81 (p-value < 0.001). This indicates evidence of a regression relationship between the dependent variable $ÄPC_{m/c}$ and the independent variables $Ṕ F_{m/c}$, $Ï_{m/c}$, $Ï_{thdf}$, $Ï_{ub}$, and $Ṽ_{ub}$ combined.

Individual coefficients contributed meaningful information in the prediction of $ÄPC_{m/c}$ (see Table 10 for O-5). The test statistics showed t-values of $Ṕ F_{m/c}$, $Ï_{m/c}$, $Ï_{thdf}$, $Ï_{ub}$, and

$\hat{V}_{ub}$ at α = 0.05. Therefore, $PF_{m/c}$, $I_{m/c}$, I_{thdf}, I_{ub}, and $\hat{V}_{ub}$ were individually useful in the prediction of $APC_{m/c}$. The coded coefficients in Table 10 reveal that, for machining operation O-5, the predictor with the highest impact on the dependent variable $APC_{m/c}$ was $I_{m/c}$ (1211), followed by $PF_{m/c}$ (1108.4), I_{ub} (367), I_{thdf} (218.9), and $\hat{V}_{ub}$ (−183.9). The negative sign indicates that the predictor $\hat{V}_{ub}$ had the highest negative effect on consumption of $APC_{m/c}$. The value of the VIF (variance inflation factor) in Table 10 for O-5 for predictors $\hat{V}_{ub}$, I_{thdf}, and $PF_{m/c}$ was less than 5. This indicates that there was no significant multicollinearity between these significant predictors. However, for the predictors I_{ub} and $I_{m/c}$, the value of VIF was greater than 5, which indicates slight multicollinearity for these predictors.

A look at the main effects plots for $APC_{m/c}$ in Figure 8a also validates the above result. The slope of significant predictors versus $APC_{m/c}$ indicates that, in this machining operation (O-5), $I_{m/c}$ had a maximum impact on $APC_{m/c}$, followed by $PF_{m/c}$, I_{ub}, and I_{thdf}. The plots also show that $\hat{V}_{ub}$ had a negative slope.

For O-5, the contour plots of $I_{m/c}$, $PF_{m/c}$, and $APC_{m/c}$ in Figure 8c indicate the maximum impact of Im/c and $PF_{m/c}$ on $APC_{m/c}$ as the number of contour lines representing different ranges of $APC_{m/c}$ consumption was greater. The contour plot between $I_{m/c}$ and I_{thdf} indicates that both parameters were significant, but their impact on $APC_{m/c}$ was not as substantial as $I_{m/c}$ and $PF_{m/c}$. The impact of I_{thdf} and $\hat{V}_{ub}$ on $APC_{m/c}$ was the least significant.

3.6. Comparative Analysis of Modeling

In order to establish the impact of significant electric parameters of estimated active power consumption of machining operations, the predicted results of equations developed with regression modeling for machining operations O-1 to O-5 were compared in this section with a standard equation of power for three-phase supply, as shown in Equation (12). Lastly, the experimental observations and predicted results from regression models and standard Equation (12) were compared in terms of absolute error calculated using Equation (13) and relative error (%) calculated using Equation (14) [55].

$$P = \sqrt{3}\hat{V}_{av}I_{m/c}\text{Cos}\phi. \quad (12)$$

$$\text{Absolute error} = |\text{Experimental value} - \text{Predicted value}|. \quad (13)$$

$$\text{Relative error (\%)} = \frac{|\text{Experimental value} - \text{Predicted value}|}{\text{Experimental value}} \times 100. \quad (14)$$

The absolute error and relative error for experimental (Exp.) active power and that predicted by standard Equation (12) (i.e., Std. Equation) are shown in Table 11 for machining operations O-1 to O-5. The absolute error and relative error for experimental active power and that predicted by regression models (Reg. Mod.) using Equations (7) to (11) are shown in Table 12 for machining operations O-1 to O-5. The average active power consumed during each of the machining operations was noted with the help of a power quality analyzer, denoted as $APC_{m/c}$ (Exp.). This experimental value was also considered the true value of the power. The average active power was then calculated using the standard Equation (12), denoted as $APC_{m/c}$ (Pred.). The average active power was also estimated from the regression model for each machining operation, denoted as $APC_{m/c}$ (Pred.) Reg. Mod.

Table 11. Active power determined using standard equation and measured by power analyzer.

Machining Operation	Avg. $\hat{V}_{av}$	Avg. $PF_{m/c}$	Avg. $\ddot{I}_{m/c}$	$\ddot{A}PC_{m/c}$ (W) (Exp.)	$\ddot{A}PC_{m/c}$ (Pred.) Std. Equation	Abs. Error Std. Equation	Relative Error
O-1	415.500	0.673	3.986	1942.203	1930.828	11.375	0.586
O-2	409.706	0.667	4.739	2302.782	2243.197	59.585	2.588
O-3	415.234	0.684	7.386	3685.243	3633.658	51.585	1.400
O-4	416.825	0.645	3.459	1528.342	1610.101	81.759	5.350
O-5	426.704	0.735	5.638	2942.897	3061.838	118.941	4.042

Table 12. Active power determined using regression equation and measured by power analyzer.

Machining Operation	Avg. $\hat{V}_{ub}$	Avg. $\hat{V}_{thdf}$	Avg. $\ddot{I}_{ub}$	Avg. $\hat{V}_{av}$	Avg $\ddot{I}_{thdf}$	Avg. $PF_{m/c}$	Avg. $\ddot{I}_{m/c}$	$\ddot{A}PC_{m/c}$ (Exp.)	$\ddot{A}PC_{m/c}$ (Pred.) Reg. Mod.	Abs. Error Reg. Mod.	Relative Error
O-1	2.600	3.626	39.887	415.500 *	40.801 *	0.673 *	3.986 *	1942.203	1941.442	0.761	0.039
O-2	1.655	6.869	35.751 *	409.706 *	42.887	0.667 *	4.739 *	2302.782	2302.557	0.225	0.010
O-3	0.405 *	2.260	10.958	415.234	40.800	0.684 *	7.386 *	3685.243	3685.243	0.000	0.000
O-4	0.238	2.263 *	19.060	416.825	43.767 *	0.645 *	3.459 *	1528.342	1528.332	0.010	0.001
O-5	0.288 *	6.350	19.698 *	426.704	51.975 *	0.735 *	5.638 *	2942.897	2942.847	0.050	0.002

* Significant predictors as per developed regression models (Equations (7) to (11)).

Figure 9a represents the machining operation along the *x*-axis, relative error along the primary *y*-axis, and the absolute error along the secondary *y*-axis. The relative error between the values of active power obtained from the power analyzer and those calculated using the standard Equation (12) is illustrated using a bar chart. The minimum relative error was 0.586 for machining operation O-1, and the maximum relative error was 5.350 for O-4.

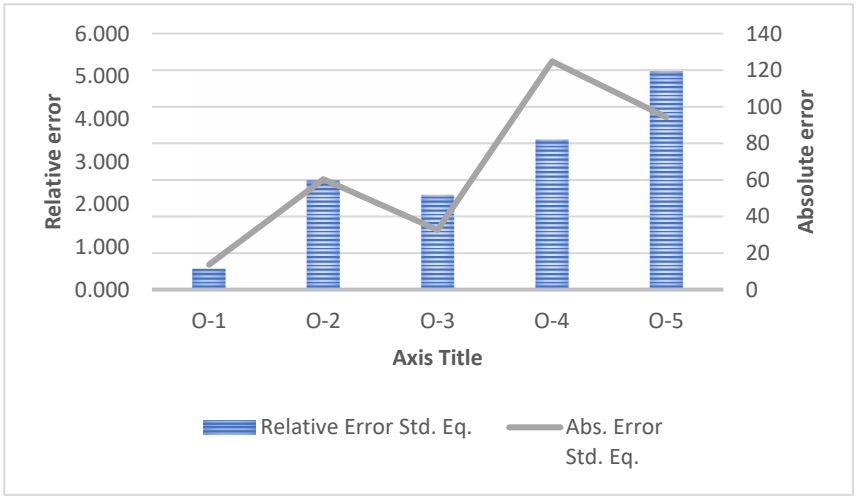

(**a**)

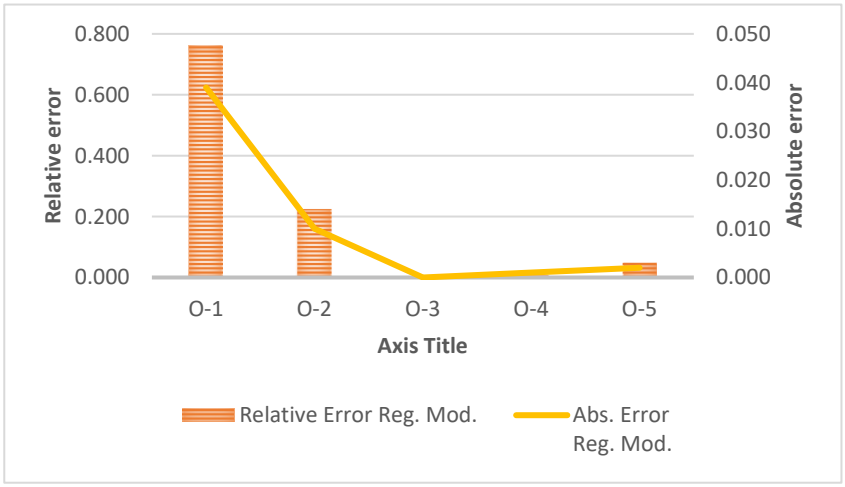

(**b**)

Figure 9. (**a**). Relative and absolute error of experimental and standard equation values. (**b**) Relative and absolute error of experimental and regression equation values.

Figure 9b shows that the relative error was minimum for O-3 (0.000) and maximum for O-1 (0.011). Figure 9 indicates the comparison between the relative errors obtained for power estimation using the standard Equation and regression models for each machining operation. It is visible that both the absolute error and the relative error were more significant in magnitude when the standard Equation (12) was used to estimate the active power. However, they become negligible when power was computed using the regression models considering the significant electric parameters. This indicates that electric parameters influence the active power and play a decisive role in gauging the magnitude of the active power consumed during the machining operation.

The regression models validate that electric parameters significantly impact the power consumption of a machining operation. It was observed that the average current had the most significant impact on electrical power consumption, followed by the power factor. Therefore, the average current consumption and power factor need to be monitored to reduce electric power consumption during the machining process.

Other electric parameters impacting power consumption are the current total harmonic distortion factor and current unbalance. Their impact was less as compared to the average current and power factor. These parameters have not been researched much. Their impact is comparatively new. There is a need to study the impact of these parameters on electrical power consumption. As a result, they were considered in the analysis. It was also observed that the average value of the power factor for different machining processes varied between 0.61 and 0.71. This value is low and needs to be improved.

It was further observed that, even for the same machining process and repetitive cuts, the significance of electric parameters concerning power consumption changed. This could have been because the electrical power being consumed by machine tools is a dynamic quantity. The working of other machine tools on the shop floor of an industry may affect the electric parameters from time to time. It is not easy to insulate a particular machine tool from the effect of other machines consuming power.

4. Hybrid Decision-Making Methodology

This section is dedicated to prioritizing the considered machining operations on the basis of energy consumption. The term "prioritization" refers to ranking the five different machining operations used in the industry. The ranks were assigned to the machining operations while considering energy consumption responses, as well as electric parameters. As a result, the user, engineer, or manager can quickly identify the machining operation consuming maximum energy. Consequently, the machining operation consuming maximum energy can be optimized on a priority basis.

Earlier regression modeling was completed to find the significant electric parameters affecting the active power consumption in the machining operation. The significant energy consumption responses and electric parameters were defined in Section 2.1. The energy responses active power, active energy, specific energy consumption, and energy efficiency were considered for decision making to prioritize the different machining operations studied in the industry. The significant electric parameters considered in the decision matrix for prioritizing machining operations were the power factor, average current, current total harmonic distortions, and current unbalance. These parameters were considered because of their significant impact on active power consumption. This was evident from the values of the coded coefficients observed during regression modeling of machining operations O-1 to O-5 (see Table 10). The electric parameters such as the average voltage, voltage unbalance, and voltage total harmonic distortion factor had a negligible impact on power consumption. In some cases, it was also negative. Moreover, these parameters were found to be nonsignificant in all the considered machining operations. As a result, they were not considered in the decision matrix.

A hybrid decision-making technique was utilized, based on the Technique for Order Preference by Similarity to Ideal Solution (TOPSIS). It was employed to convert multiple performances into a single score called the multiple composite score (MCS). The TOPSIS assumes that the chosen alternative will have the shortest Euclidean divergence from the ideal positive solution and the most divergence from the ideal negative solution. The steps described below are usually employed in this technique [37,56,57].

Step 1: Identification of study objectives and responses. The decision pattern was considered as per Equation (15). Every row of the decision matrix (DM) was assigned to each experiment number and column to one response, i.e., ÄPC$_{m/c}$, ÄEC$_{m/c}$, ĖĖ$_{ṁ}$, and ṔF$_{m/c}$. q_{ij} is an element of the decision matrix 'DM' [q_{ij}; i = 1, 2, …, a number of experiments (*n*), j = 1, 2, …., number of responses (m)] which is input.

$$DM=\begin{bmatrix} q_{11} & q_{12} & \cdots & q_{1j} & \cdots & q_{1m} \\ q_{21} & q_{22} & \cdots & q_{2j} & \cdots & q_{2m} \\ \cdots & \cdots & \cdots & \cdots & \cdots & \cdots \\ q_{i1} & q_{i2} & \cdots & q_{ij} & \cdots & q_{im} \\ \cdots & \cdots & \cdots & \cdots & \cdots & \cdots \\ q_{n1} & q_{n2} & \cdots & q_{nj} & \cdots & q_{nm} \end{bmatrix}. \quad (15)$$

Step 2: The vector normalization obtained the normalized DM (M_{ij}) as per Equation (16).

$$M_{ij}=\left[\frac{q_{ij}}{\left[\sum_{i=1}^{n} q_{ij}^{2}\right]^{\frac{1}{2}}}\right]. \quad (16)$$

Step 3: The weights (w_j) of significance were assigned to the responses, w_j; j = 1, 2…… m, such that $\sum w_j = 1$. In the present study, three methods of weight assignment were used: identical, objective, and subjective preferences.

- Equal-weights method

In this technique, weights were attained, dividing one by the total number of responses, as per Equation (17).

$$w_j = \frac{1}{m}. \quad (17)$$

Since there eight responses in the present case, the weight assigned to each response was 0.125 ($w_j = 12.5\%$).

- Entropy-weights method

Weights are established without considering the influence of decision-makers by using probability and measuring uncertain information. The fundamental principle of weight estimation with entropy is that a higher weight index value is more efficient than a lower index value [58]. The DM listed in Equation (15) is normalized using Equation (18) for a beneficial response, e.g., power factor, and Equation (19) for a nonbeneficial reaction, e.g., energy consumption by the linear normalization technique; it is noticeable that the normalized decision matrix $NDM_{ij} \in [0, 1]$ [59].

The probability of the response (Pr_{ij}) to happen is computed suing Equation (20), and Equation (21) is utilized to attain the entropy (En_j) of the *j*th response. In Equation (21), $Y = \frac{1}{\log_e(n)}$ is a stable expression, n is the number of experiments, and the value of En_j lies between zero and one.

Equation (22) is utilized to compute the degrees of divergence (Div_j), and Equation (23) obtains the entropy weight (E_w) of the *j*th response.

$$NDM_{ij} = \frac{q_{ij}}{Max q_{ij}} \text{ (Beneficial).} \quad (18)$$

$$NDM_{ij} = \frac{Min q_{ij}}{q_{ij}} \text{ (Nonbeneficial).} \quad (19)$$

$$Pr_{ij} = \frac{NDM_{ij}}{\sum_{i=1}^{n} NDM_{ij}}. \quad (20)$$

$$En_j = -Y \sum_{i=1}^{n} Pr_{ij} \log_e (Pr_{ij}). \quad (21)$$

$$Div_j = | 1-En_j |. \quad (22)$$

$$Ew_j = \frac{Div_j}{\sum_{j=1}^{m} Div_j}. \quad (23)$$

- Analytic Hierarchy Process (AHP) weights

This method attains weights for responses with the consent of the decision-maker. In the end, a nine-point inclination scale is used to obtain the relative importance of responses by building a pairwise comparison matrix [60].

Assuming m responses (R_m), a pairwise comparison matrix ($R_{m\times m}$) can be built, Equation (24), for the pairwise comparison of response (R_i) with a response (R_j). To attain the elements of $R_{m\times m}$, the suitable comparative significance can be assigned to every row response (R_1, R_2, ..., R_m) by comparing the value with the response from every column (R_1, R_2, …, R_m). In $R_{m\times m}$, the value of $r_{ij} = 1$ for i = j, i.e., a response compared with itself is always equal to 1, and other leftover elements of the $R_{m\times m}$ (for $i \neq j$) are the reciprocal of the equivalent component, e.g., $r_{12} = 1/r_{21}$. Consequently, the first diagonal entries of $R_{m\times m}$ are equal

answers of responses. Half of the remaining entries are reciprocal of the equivalent elements to 1, and the other half are agreed by contrasting the corresponding elements. The relative normalized weight ($\dot{w}_j$) of every response is obtained by taking the ratio of the geometric mean $\mathcal{G}M$ of the equivalent row in the $B_{m\times m}$ comparison to the sum of the geometric means of all the rows (see Equations (25) and (26)).

Equation (27) yields the consistency index (ĆÍ), where λ_{max} is the maximum eigenvalue of $B_{m\times m}$. λ_{max} is obtained by taking the average value of the sum of the matrix product of the pairwise $B_{m\times m}$ comparison and $\dot{w}_j$ vectors and dividing by the relative normalized weight of the equivalent response. A lower value of ĆÍ, denotes a lower variation from the consistency. Equation (28) provides the consistency ratio (ĆŔ). In Equation (28), ŔÍ is the random index value (see [60]). Generally, a ĆŔ of 0.10 or less is considered adequate, and it imitates an informed opinion attributable to the acquaintance of a market analyst concerning the problem of study.

$$\begin{array}{l}\text{Response (j)} \quad R_1 \quad R_2 \quad -- \quad R_j \quad -- \quad R_m. \\ \text{(i)}\end{array}$$

$$R_{m\times m} = \begin{array}{c} R_1 \\ R_2 \\ -- \\ R_i \\ -- \\ R_m \end{array} \begin{bmatrix} 1 & r_{12} & -- & r_{1j} & -- & r_{1m} \\ r_{21} & 1 & -- & r_{2j} & -- & r_{2m} \\ -- & -- & -- & -- & -- & -- \\ r_{i1} & r_{i2} & -- & r_{ij} & -- & r_{im} \\ -- & -- & -- & -- & -- & -- \\ r_{m1} & r_{m2} & -- & r_{mj} & -- & 1 \end{bmatrix}. \tag{24}$$

$$\mathcal{G}M = \left[\prod_{j=1}^{m} r_{ij}\right]^{\frac{1}{m}}. \tag{25}$$

$$\dot{w}_j = \mathcal{G}M / \sum_{i=1}^{m} \mathcal{G}M. \tag{26}$$

$$ĆÍ = \frac{\lambda_{max} - m}{m - 1}. \tag{27}$$

$$ĆŔ = \frac{ĆÍ}{ŔÍ}. \tag{28}$$

Step 4: The weighted normalized matrix ($\hat{W}\dot{Z}_{ij}$) was obtained by multiplying the columns of M_{ij} with their respective assigned weight, $\dot{w}_j$. Subsequently, $\hat{W}\dot{Z}_{ij}$ was attained using Equation (29).

Step 5: In this stage, it was necessary to find out the ideal best (Z^+) and ideal worst (Z^-) solutions with the help of Equations (30) and (31), respectively. Here, Z^+ and Z^- solutions were the largest and smallest values amongst all response values, respectively. In Equation (30), j and j' are related to the beneficial (m) and nonbeneficial attributes (m'), respectively.

Step 6: Separation measures (Sep_m) were prepared on the basis of Euclidean distance (see Equations (32) and (33)).

Step 7: The relative closeness or 'MCS' of all experiments was computed, i.e., alternatives representing the ideal resolution using Equation (34).

$$\hat{W}\dot{Z}_{ij} = \left[\dot{w}_j \times M_{ij}\right]. \tag{29}$$

$$Z_j^+ = \{\text{best } (\hat{W}\dot{Z}ij)\}_{i=1}^{n}. \tag{30}$$

$$Z^{+} = \left\{Z_1^{+}, Z_2^{+}, \ldots, Z_j^{+}, \ldots Z_m^{+}\right\}.$$

$$Z_{j'}^{-} = \{\text{worst } (\hat{W}\dot{Z}_{ij'})\}_{i=1}^{n}.$$

$$Z^{-} = \left\{Z_1^{-}, Z_2^{-}, \ldots, Z_{j'}^{-}, \ldots Z_{m'}^{-}\right\}. \quad (31)$$

$$Sep_i^{+} = \{\sum_{j=1}^{m} (Z_{ij} - Z_j^{+})^2\}^{0.5}. \quad (32)$$

$$Sep_i^{-} = \{\sum_{j'=1}^{m'} (Z_{ij} - Z_{j'}^{-})^2\}^{0.5}. \quad (33)$$

$$MCS = \frac{Sep_i^{-}}{Sep_i^{+} + Sep_i^{-}}. \quad (34)$$

Step 8: The methods to select the final ranks of alternatives based on individual results from different MCDM weights are described below.

Step 9: Degree of Membership (DoM)

Let $\mathcal{R}_{xy}$ be the rank matrix of the y^{th} alternative using the x^{th} MCDM method (x =1, 2, ..., k, y =1, 2, ..., t), where k is the number of MCDM methods and t is the number of alternatives.

Step 9.1: Constitute the rank matrix $\mathcal{R} = (r_{xy})$ k × t.

Step 9.2: Calculate the values of the rank state variables; x =1, 2, ..., k, y = 1, 2, ..., t z = 1, 2, ..., t from the rank matrix $\mathcal{R} = (r_{xy})$ k × t, using Equation (35).

Step 9.3: Constitute rank frequency number matrix F = (f_{yz}) txt, where f_{yz} is the rank frequency number that the rank of the y^{th} alternative is the z^{th} place according to different MCDM methods, and f_{yz} is expressed as Equation (36).

Step 9.4: Constitute the membership degree matrix $\varphi = (\varphi_{yz})$ txt, where φ_{yz} is the membership degree that the rank of the y^{th} alternative belongs to the z^{th} place according to different MCDM methods, and φ_{yz} is expressed as Equation (37).

The y^{th} row ($\varphi_{y1}, \varphi_{y1}, \ldots, \varphi_{yt}$) of the membership degree matrix $\varphi = (\varphi_{yz})$ txt represents the degree that the rank of y^{th} alternative belongs to k places, where

$0 \le \varphi_{yz} \le 1$ and $\sum_{z=1}^{k} \varphi_{yz} = 1$.

Step 9.5: Calculate the final rank index $\mathcal{P}_y$ of the y^{th} alternative ($y = 1,2,\ldots,t$), where $\mathcal{P}_y$ is calculated using Equation (38).

Step 9.6: Determine final ranks r01, r02, …, r0t of the operations in ascending order based on the values of $\mathcal{P}_1, \mathcal{P}_2, \mathcal{P}_3, \ldots \mathcal{P}_t$.

$$\delta_{yz}^{(x)} = \begin{cases} 1\,; & r_{xy} = z \\ 0\,; & r_{xy} \neq z \end{cases} \quad (x = 1, 2, \ldots, k, \quad y = 1, 2, \ldots, t \quad z = 1, 2, \ldots, t. \quad (35)$$

$$f_{yz} = \sum_{x=1}^{k} \delta_{yz}^{(x)} \; (y = 1, 2, \ldots, t \; z = 1, 2, \ldots, t). \quad (36)$$

$$\varphi_{yz} = f_{yz}/k \; (y = 1, 2, \ldots, t \; z = 1, 2, \ldots, t.) \quad (37)$$

$$\mathcal{P}_y = \sum_{z=1}^{t} z \cdot \varphi_{yz}. \quad (38)$$

Table 13 describes the active power consumption by the machine (ÄPC$_{m/c}$) in kW, active energy consumption by the machine (ÄEC$_{m/c}$) in kWh, energy efficiency (ĖĖ$_{ŋ}$) as a percentage, specific energy consumption (ş) in kJ/cm^3 for the power factor (ƤF$_{m/c}$), the average current of the actual or machining cut (Ï$_{m/c}$) in rms, the current total harmonic distortion factor of the actual or machining cut (Ï$_{thdf}$), and the current unbalance of the actual cut (Ï$_{ub}$) using a decision matrix as per Equation (15). The normalized decision matrix was calculated as per Equation (16) and is shown in Table A1 (Appendix A). ÄPC$_{m/c}$, ÄEC$_{m/c}$, ş, Ï$_{m/c}$, Ï$_{thdf}$, and Ï$_{ub}$ were "the lower, the better" energy responses, and ĖĖ$_{ŋ}$ and ƤF$_{m/c}$ were "the higher, the better" energy responses; the calculation was done to four significant decimal places.

Table 13. Decision matrix of energy responses.

Operation	ÄPC$_{m/c}$	ÄEC$_{m/c}$	ĖĖ$_{ŋ}$	ş	ƤF$_{m/c}$	Ï$_{m/c}$	Ï$_{thdf}$	Ï$_{ub}$
O-1	1.973	0.084	25.619	15.308	0.677	4.027	40.898	40.316
O-2	2.321	0.067	38.209	12.207	0.675	4.719	40.965	35.67
O-3	3.707	0.077	40.260	14.097	0.687	7.405	41.435	10.94
O-4	1.542	0.033	30.303	31.548	0.647	3.478	43.673	18.583
O-5	2.975	0.053	43.396	13.343	0.738	5.691	51.447	19.42

Estimation of weights for responses

- Equal-Weights Method

The weights for responses were estimated using the equal-weights method as per Equation (3), revealing 12.5% or 0.125 each.

- Entropy-Weights Method

Equations (18) and (19) yielded the normalized decision matrix (NDM$_{ij}$) for computation of entropy weights for beneficial and by the nonbeneficial responses, respectively. The NDM$_{ij}$ for entropy-weights is shown in Table A1. The probability of the response (Pr_{ij}) was computed using Equation (20), and the result is shown in Table A2. The entropy (En_j) of the response was calculated using Equation (21), while the degrees of divergence (Div_j) and entropy-weights (Ew_j) were calculated using Equations (22) and (23), respectively. The attained results are shown in Table 14.

Table 14. Entropy-weights computation and weights.

	ÄPC$_{m/c}$	ÄEC$_{m/c}$	ĖĖ$_{ŋ}$	ş	ƤF$_{m/c}$	Ï$_{m/c}$	Ï$_{thdf}$	Ï$_{ub}$
En_j	0.9718	0.9600	0.9890	0.9741	0.9994	0.9798	0.9978	0.9316
Div_j	0.0282	0.0400	0.0110	0.0259	0.0006	0.0202	0.0022	0.0684
Ew_j	0.1437	0.2034	0.0561	0.1321	0.0030	0.1028	0.0111	0.3481
Ew_j(%)	14.371	20.343	5.6058	13.207	0.2957	10.279	1.1134	34.806

- AHP Method

To attain AHP weights, a pairwise comparison matrix of responses was established as per Equation (24). The pairwise comparison matrix was a collective decision of the research group, as well as people from academia and industry. A questionnaire was drafted on the basis of eight energy consumption responses to get opinions from the local industry experts and people from academia. The questionnaire content was decided by selecting energy responses from the literature and assigning electric parameters based on regression modeling. Lastly, an event was arranged, and 12 experts were invited for a brainstorming session to complete a pairwise comparison matrix of energy responses. This event comprised six experts from academia and six from the industry. The final agreed pairwise comparison matrix is shown in Table 15.

Table 15. Pairwise comparison matrix.

Responses	ÄPC$_{m/c}$	ÄEC$_{m/c}$	ĖĖ$_{ή}$	ş	ƤF$_{m/c}$	Ï$_{m/c}$	Ï$_{thdf}$	Ï$_{ub}$
ÄPC$_{m/c}$	1	1/5	1/7	1/5	1/7	1/3	1/5	1/2
ÄPC$_{m/c}$	5	1	1	1	1	1/3	1/3	1
ĖĖ$_{ή}$	7	1	1	1	1	1/3	1/3	1
ş	5	1	1	1	1	3	1/2	1
ƤF$_{m/c}$	7	1	1	1	1	1/3	1/3	1
Ï$_{m/c}$	3	3	3	1/3	3	1	1/3	3
Ï$_{thdf}$	5	3	3	2	3	3	1	3
Ï$_{ub}$	2	1	1	1	1	1/3	1/3	1
Eigen Vector	0.03	0.093	0.1	0.151	0.1	0.174	0.269	0.083

The relative normalized weight and the weights of responses were computed using Equations (25) and (26), respectively. The consistency index and ratio were calculated using Equations (27) and (28), respectively. The maximum eigenvalue was λ_{max} = 8.816, and the consistency ratio CR was 8.3%. The CR was observed to be below the permitted value of 10%, indicating substantial accuracy in the decision-maker's judgment when assigning values in the matrix for pairwise comparisons. The weights of significance computed using the three different methods are listed in Table 16.

Table 16. Weights of energy responses computed using three methods.

	ÄPC$_{m/c}$	ÄEC$_{m/c}$	ĖĖ$_{ή}$	ş	ƤF$_{m/c}$	Ï$_{m/c}$	Ï$_{thdf}$	Ï$_{ub}$
Equal	12.5%	12.5%	12.5%	12.5%	12.5%	12.5%	12.5%	12.5%
Entropy	14.37%	20.34%	5.60%	13.21%	0.29%	10.27%	1.11%	34.81%
AHP	3%	9.3%	10%	15.10%	10%	17.4%	26.9%	8.3%

The normalized decision matrix for TOPSIS method calculations was obtained as per Equation (16) and is shown in Table A3. The weighted normalized matrix ($\hat{W}\dot{Z}_{ij}$) was computed using Equation (29) and is tabulated in Table A3 for equal, entropy, and AHP weights. The positive ideal (best) answer was calculated using Equation (30), and the negative ideal (worst) response was calculated using Equation (31); the attained values are depicted in Table A6 for equal, entropy, and AHP weights. Equations (32) and (33) were applied to calculate separation measures (Sep$_m$) for positive and negative answers, respectively. The evaluated responses are depicted in Table 17. The relative closeness or MCS was calculated using Equation (34), and the computed results are tabulated in Table 17. The final ranks attained using the three different weight methods are shown in Table 17.

Table 17. Separation measures and multiple composite scores (MCSs).

Operation	Equal Weights				Entropy Weights				AHP Weights			
	Sep$_i^+$	Sep$_i^-$	MCS	Rank	Sep$_i^+$	Sep$_i^-$	MCS	Rank	Sep$_i^+$	Sep$_i^-$	MCS	Rank
O-1	0.0806	0.0721	0.0341	5	0.1827	0.2555	0.0208	5	0.0573	0.0702	0.0387	3
O-2	0.0628	0.0752	0.0410	4	0.1502	0.2321	0.0289	4	0.0450	0.0697	0.0423	2
O-3	0.0733	0.0839	0.0448	3	0.0883	0.2649	0.1177	1	0.0660	0.0666	0.0335	5
O-4	0.0636	0.0890	0.0519	2	0.0754	0.2315	0.1052	2	0.0514	0.0770	0.0461	1
O-5	0.0477	0.0829	0.0526	1	0.0688	0.2102	0.0951	3	0.0476	0.0656	0.0380	4

The ranks obtained using the various weight methods were different for each machining operation. Thus, to get the final combined ranks, the degree of membership technique was applied, as shown in Step 9 of the decision-making methodology. First, the constitute rank frequency number of the machining operations from O-1 to O-5 was calculated using Equation (35), and the results are shown in Table A6. Then, a membership

degree was constituted using Equation (36). Lastly, the final rank index of each machining operation was obtained using Equation (37), as shown in Table 18. The final ranks of each machining operation were then calculated, and the results are presented in Figure 10.

Table 18. Final ranks of operations using degree of membership (DoM).

Weights	1	2	3	4	5	SUM	Rank
O-1	0.0000	0.0000	1.0000	0.0000	3.3333	4.3333	5
O-2	0.0000	0.6667	0.0000	2.6667	0.0000	3.3333	4
O-3	0.3333	0.0000	1.0000	0.0000	1.6667	3.0000	3
O-4	0.3333	1.3333	0.0000	0.0000	0.0000	1.6667	1
O-5	0.3333	0.0000	1.0000	1.3333	0.0000	2.6667	2

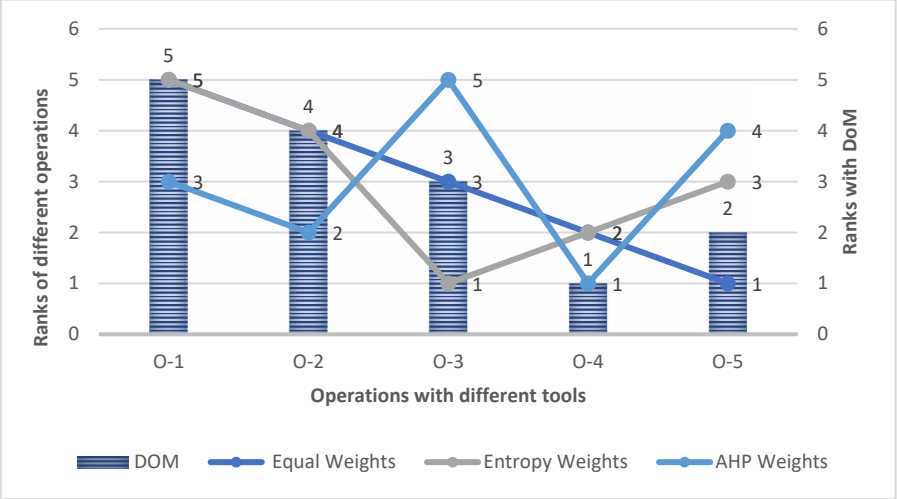

Figure 10. Ranks established using different weight methods, along with the final rank determined using a degree of membership.

Prioritizing the machining process in terms of energy consumption was conducted systematically. Machining operation O-1 emerged as the most energy-intensive process. Five machining operations O-1 to O-5 were considered, and eight response parameters were measured. The allocation of weights to responses was an important step. To rule out any bias of the researcher, three methods were employed. The first assigned equal weights to all the responses. Under this method, the reciprocal of the total number of the responses was taken, and equal weights were assigned to all the responses. The second was an objective method, i.e., the entropy weight method, in which weights were assigned without considering the researcher's input. First, the probability of the response was worked out, and then the entropy of the response was calculated. This step was followed by working out the degree of divergence and assigning entropy weights. This was a purely analytical method, and the bias of the researcher was ruled out.

The third method involved giving importance to the responses by a process of subjective preference, i.e., the AHP method. In this method, a pairwise comparison was made between identified responses. A nine-point Saaty scale was used to obtain the relative importance of responses [60]. The decision-makers were a group of experts. For example, for the present research, mechanical engineers, electrical engineers, technical experts from the concerned industry, and technical tool suppliers formed the expert group. First, the judgment values of each expert were considered. Then, the relative normalized weight and the weight of responses were calculated. In this case, the consistency ratio worked out to be 8.3%, which was less than the allowed value of 10%. This indicates precision in the decision-maker's judgment in allocating values for pairwise comparison.

Table 16 shows that the equal weights method assigned equal weights to all responses. The entropy method gave the maximum importance to the current unbalance (34.81%), followed by actual energy consumption (20.34%) and the average power consumption (14.37%). The AHP assigned maximum weight to the current total harmonic distortion factor (26.9%). Even in the multiple regression analysis, the current total harmonic distortion factor remained a significant parameter in machining operations O-1, O-2, and O-3. The second parameter to which the entropy method assigned weight was the average current (17.4%). This indicates the extreme impact of current on active power consumption.

Thus, in terms of prioritizing a machining operation based on energy consumption, rank 1 indicated the most energy-efficient machining operation, and rank 5 showed the most energy-intensive operation. It was observed that, under TOPSIS, the various weights methods graded the machining operations differently. The method of equal weights and the entropy weights method assigned rank 5 to the machining operation O-5. This indicates that machining operation 5 was the most energy-intensive process. At the same time, the method of AHP ranked machining operation O-3 as rank 5. To bring uniformity to the results and get a final combined rank, the degree of membership (DOM) was implemented. The results are presented in Table 18 and highlighted in Figure 10.

Machining operation O-1 emerges as the most energy-intensive process. O-1 is a machining process in which drilling occurs with the help of a high-speed steel (HSS) drill of diameter 16 mm and flute length 110 mm. The drilled hole depth is 77 mm. The spindle RPM is 450, and the feed rate is 70 mm/min (see Table 3). The process takes 154 s to complete, which is a lot of time. Hence, the energy consumed is more. This process will be looked into, and possibilities for a reduction in energy consumption will be suggested with the help of experimentation. This becomes a scope for future research.

5. Conclusions

This study presented a practical technique for enhancing the sustainability of machining operations in an industry. The article emphasized the significance of electric parameters in the active power consumption of machining operations. It encompassed a systematic approach for the identification of the most energy-intensive machining operation. Based on the critical outcome, the following conclusions were drawn:

- The quality of the power supplied to the machine tool seems to be affected by the concurrent functioning of the other machine tools in the surrounding area of the machine shop. This is evident from the fact that different electric parameters become significant at different times in the power consumption of a machining operation examined on the same shop floor of the industry. Therefore, the quality of power being supplied to the machine tool needs to be monitored and corrected to lower power consumption.
- Multiple regression analysis revealed that, out of the seven electric parameters considered, the rms values of the current and the power factor emerged as significant in all five machining operations. The current total harmonic distortion factor appeared significant in the three machining operations (O-1, O-4, and O-5). Current unbalance, the rms value of voltage, and voltage unbalance were significant in two machining operations each (O-2 and O-5, O-1 and O-2, and O-3 and O-5, respectively). The voltage total harmonic distortion factor was significant in only a single machining operation (O-4).
- The values of the coded coefficients of regression models revealed the relative impact of significant electric parameters on active power consumption. It was observed that the rms value of the current had the maximum direct impact, followed by the power factor. Therefore, their optimization would lead to a maximum reduction in electric power and energy. These factors were followed by the current unbalance, which also had a direct impact on power consumption. The rms value of voltage ranked last,

with a small positive impact, whereas the voltage unbalance and the total harmonic distortion factor negatively affected the power consumption. To reduce the power consumption of a machining operation, it is imperative to assess the significance of electric parameters and evaluate their relative importance.

- The maximum absolute error in the estimation of active power using the standard power equation was 118.941 for machining operation O-5, but that with the developed regression model was 0.05. Similarly, the maximum relative error using the standard power equation was 5.350 for O-4 compared to 0.001 using the developed regression model. The R-squared value was more than 98% for O-1 to O-4 and 93% for O-5 for the developed models. This proves the results are theoretically correct.
- The TOPSIS equal-weights method identified machining operation O-1 as the most energy-intensive and O-5 as the least energy-intensive. With the assistance of the entropy weights without the decision maker's input, the same technique classified machining operation O-1 as the most energy-intensive but O-3 as the least energy-intensive process. The AHP weights method with the decision-maker's input ranked O-5 as the maximum and O-4 as the minimum energy consumption. Furthermore, the degree of membership (DoM) approach was employed to establish the final conjoined ranks. Machining operation O-1 was the most energy-intensive, followed by O-2, O-3, O-5, and O-4.
- The awareness of the importance of electric parameters in the active power consumption of machining processes and the identification of the energy-intensive machining operation benefit researchers and the industry in reducing energy consumption and minimizing the impact of carbon dioxide emissions in the industry environment.
- The most energy-intensive machining operation identified, i.e., O-1, a drilling process, needs to be optimized for minimum energy consumption. In addition, research is required to investigate or explore why some electric parameters become significant and others do not for the machine tools and machining processes conducted on the same shop floor. Furthermore, some electric parameters have positive and small negative impacts on the machining operation's power consumption and need to be investigated.

Author Contributions: Conceptualization, A.S.S. and R.K.; methodology, R.K. and S.S.; software, A.S.S., R.K., S.S., D.Y.P. and K.G.; validation, K.G., A.S.S. and R.K.; formal analysis, R.K.; investigation, A.S.S. and R.K.; resources, A.S.S.; data curation, A.S.S.; writing—original draft preparation, A.S.S., R.K., K.G. and D.Y.P.; writing—review and editing, A.S.S., R.K. and S.S.; visualization, S.S., D.Y.P. and K.G.; supervision, S.S.; project administration, A.S.S. All authors have read and agreed to the published version of the manuscript.

Funding: Not applicable.

Institutional Review Board Statement: Not applicable.

Informed Consent Statement: Not applicable.

Data Availability Statement: Not applicable.

Acknowledgments: The authors express deep gratitude to I. K. Gujral Punjab Technical University, Kapurthala-Jalandhar (Punjab), India, for providing the facilities to carry out this research work. Furthermore, the authors earnestly thank the joint MD of Auto International, Village Mangarh on Kohara, Machhiwara Road, Ludhiana-Punjab (India), Rajan Mittal, and Rohit Gupta for permitting observations and experimentation in the machine shop of their industry. The authors also thank Kuldeep Singh, the production supervisor.

Conflicts of Interest: The authors declare no conflicts of interest.

Nomenclature

Abbreviations	**Acronym**	**Units**
Machining Time	$t_{m/c}$	seconds (s)
Active power consumption air cut	APC_{air}	kilowatt (kW)
Active power consumption by machine	$APC_{m/c}$	kilowatt (kW)
Active energy consumption air cut	AEC_{air}	kilowatt hour (kWh)
Active energy consumption by machine	$AEC_{m/c}$	kilowatt hour (kWh)
Energy efficiency	E_η	No units
Specific energy consumption	u	kilojoule/cm^3
Power factor	$PF_{m/c}$	No units
Average current (rms)	$I_{m/c}$	ampere (A)
Current total harmonic distortion factor	I_{thdf}	(%)
Current unbalance	I_{ub}	(%)
Average voltage (rms)	V_{av}	volt
Voltage total harmonic distortion factor	V_{thdf}	(%)
Voltage unbalance	V_{ub}	(%)
Air cut	AC	No unit
Actual cut	ACT	No unit
p-Value	P	No unit
Volume of material removed	V	cm^3
Cutting speed	V_c	m/min
Depth of cut	d	mm
Feed rate	f_d	mm/min
Specific cutting energy	Se	kJ/cm^3
Tool wear	T_w	mm
Material removal rate	ω	cm^3/min

Appendix A

Table A1. Normalized decision matrix (entropy method).

Operation	**$APC_{m/c}$**	**$AEC_{m/c}$**	**E_η**	**u**	**$PF_{m/c}$**	**$I_{m/c}$**	**I_{thdf}**	**I_{ub}**
O-1	0.7814	0.3929	0.5904	0.7974	0.9169	0.8638	1.0000	0.2714
O-2	0.6644	0.4925	0.8805	1.0000	0.9146	0.7370	0.9984	0.3067
O-3	0.4160	0.4286	0.9277	0.8659	0.9309	0.4697	0.9870	1.0000
O-4	1.0000	1.0000	0.6983	0.3869	0.8767	1.0000	0.9365	0.5887
O-5	0.5183	0.6226	1.0000	0.9149	1.0000	0.6111	0.7950	0.5633

Table A2. Probability of responses (entropy method).

Operation	**$APC_{m/c}$**	**$AEC_{m/c}$**	**E_η**	**u**	**$PF_{m/c}$**	**$I_{m/c}$**	**I_{thdf}**	**I_{ub}**
O-1	0.2312	0.1338	0.1441	0.2011	0.1977	0.2346	0.2120	0.0994
O-2	0.1966	0.1677	0.2149	0.2522	0.1972	0.2002	0.2117	0.1123
O-3	0.1231	0.1459	0.2264	0.2184	0.2007	0.1276	0.2093	0.3663
O-4	0.2959	0.3405	0.1704	0.0976	0.1890	0.2716	0.1985	0.2156
O-5	0.1533	0.2120	0.2441	0.2307	0.2156	0.1660	0.1685	0.2063

Table A3. Normalized decision matrix (TOPSIS).

Operation	**$APC_{m/c}$**	**$AEC_{m/c}$**	**E_η**	**u**	**$PF_{m/c}$**	**$I_{m/c}$**	**I_{thdf}**	**I_{ub}**
Equal weights								
O-1	0.3372	0.5746	0.3168	0.3654	0.4415	0.3430	0.4169	0.6592
O-2	0.3966	0.4583	0.4725	0.2914	0.4404	0.4020	0.4176	0.5833

O-3	0.6334	0.5267	0.4979	0.3365	0.4483	0.6308	0.4224	0.1789
O-4	0.2635	0.2257	0.3748	0.7530	0.4222	0.2963	0.4452	0.3039
O-5	0.5083	0.3625	0.5367	0.3185	0.4815	0.4848	0.5245	0.3176
Entropy weights								
O-1	0.3372	0.5746	0.3168	0.3654	0.4415	0.3430	0.4169	0.6592
O-2	0.3966	0.4583	0.4725	0.2914	0.4404	0.4020	0.4176	0.5833
O-3	0.6334	0.5267	0.4979	0.3365	0.4483	0.6308	0.4224	0.1789
O-4	0.2635	0.2257	0.3748	0.7530	0.4222	0.2963	0.4452	0.3039
O-5	0.5083	0.3625	0.5367	0.3185	0.4815	0.4848	0.5245	0.3176
AHP weights								
O-1	0.3372	0.5746	0.3168	0.3654	0.4415	0.3430	0.4169	0.6592
O-2	0.3966	0.4583	0.4725	0.2914	0.4404	0.4020	0.4176	0.5833
O-3	0.6334	0.5267	0.4979	0.3365	0.4483	0.6308	0.4224	0.1789
O-4	0.2635	0.2257	0.3748	0.7530	0.4222	0.2963	0.4452	0.3039
O-5	0.5083	0.3625	0.5367	0.3185	0.4815	0.4848	0.5245	0.3176

Table A4. Weighted normalized matrix (ŴŻ$_{ij}$) TOPSIS.

Operation	**ÄPC$_{m/c}$**	**ÄEC$_{m/c}$**	**ĖĖ$_{\eta}$**	**ş**	**ƤF$_{m/c}$**	**Ï$_{m/c}$**	**Ï$_{thdf}$**	**Ï$_{ub}$**
Equal weights								
O-1	0.0421	0.0718	0.0396	0.0457	0.0552	0.0429	0.0521	0.0824
O-2	0.0496	0.0573	0.0591	0.0364	0.0551	0.0502	0.0522	0.0729
O-3	0.0792	0.0658	0.0622	0.0421	0.0560	0.0789	0.0528	0.0224
O-4	0.0329	0.0282	0.0468	0.0941	0.0528	0.0370	0.0557	0.0380
O-5	0.0635	0.0453	0.0671	0.0398	0.0602	0.0606	0.0656	0.0397
Entropy weights								
O-1	0.0485	0.1169	0.0178	0.0483	0.0013	0.0353	0.0046	0.2295
O-2	0.0570	0.0932	0.0265	0.0385	0.0013	0.0413	0.0046	0.2030
O-3	0.0910	0.1071	0.0279	0.0444	0.0013	0.0648	0.0047	0.0623
O-4	0.0379	0.0459	0.0210	0.0994	0.0012	0.0305	0.0050	0.1058
O-5	0.0731	0.0737	0.0301	0.0421	0.0014	0.0498	0.0058	0.1105
AHP weights								
O-1	0.0101	0.0534	0.0317	0.0365	0.0667	0.0597	0.1122	0.0547
O-2	0.0119	0.0426	0.0473	0.0291	0.0665	0.0699	0.1123	0.0484
O-3	0.0190	0.0490	0.0498	0.0336	0.0677	0.1098	0.1136	0.0148
O-4	0.0079	0.0210	0.0375	0.0753	0.0637	0.0516	0.1198	0.0252
O-5	0.0152	0.0337	0.0537	0.0318	0.0727	0.0844	0.1411	0.0264

Table A5. Ideal positive and negative results.

	ÄPC$_{m/c}$	**ÄEC$_{m/c}$**	**ĖĖ$_{\eta}$**	**ş**	**ƤF$_{m/c}$**	**Ï$_{m/c}$**	**Ï$_{thdf}$**	**Ï$_{ub}$**
Equal weights								
Ideal positive	0.0329	0.0282	0.0671	0.0364	0.0602	0.0370	0.0521	0.0224
Ideal negative	0.0792	0.0718	0.0396	0.0941	0.0528	0.0789	0.0656	0.0824
Entropy weights								
Ideal positive	0.0379	0.0459	0.0301	0.0385	0.0014	0.0305	0.0046	0.0623
Ideal negative	0.0910	0.1169	0.0178	0.0994	0.0012	0.0648	0.0058	0.2295
AHP weights								
Ideal positive	0.0079	0.0210	0.0537	0.0291	0.0727	0.0516	0.1122	0.0148
Ideal negative	0.0190	0.0534	0.0317	0.0753	0.0637	0.1098	0.1411	0.0547

Table A6. Frequency of ranks according to DoM.

Ranks	1	2	3	4	5
O-1	0	0	1	0	2
O-2	0	1	0	2	0
O-3	1	0	1	0	1
O-4	1	2	0	0	0
O-5	1	0	1	1	0

References

1. Aktar, M.A.; Alam, M.M.; Al-Amin, A.Q. Global economic crisis, energy use, CO_2 emissions, and policy roadmap amid COVID-19. *Sustain. Prod. Consum.* **2021**, *26*, 770–781, doi:10.1016/j.spc.2020.12.029.
2. Sutrisno, A.; Nomaler, Ö.; Alkemade, F. Has the global expansion of energy markets truly improved energy security? *Energy Policy* **2021**, *148*, 111931, doi:10.1016/j.enpol.2020.111931.
3. Bogdanov, D.; Ram, M.; Aghahosseini, A.; Gulagi, A.; Oyewo, A.S.; Child, M.; Caldera, U.; Sadovskaia, K.; Farfan, J.; De Souza Noel Simas Barbosa, L.; et al. Low-cost renewable electricity as the key driver of the global energy transition towards sustainability. *Energy* **2021**, *227*, 120467, doi:10.1016/j.energy.2021.120467.
4. Zhang, Y. Review of recent advances on energy efficiency of machine tools for sustainability. *Proc. Inst. Mech. Eng. Part B J. Eng. Manuf.* **2014**, *229*, 2095–2108, doi:10.1177/0954405414539490.
5. Yoon, H.-S.; Kim, E.-S.; Kim, M.-S.; Lee, J.-Y.; Lee, G.-B.; Ahn, S.-H. Towards greener machine tools—A review on energy saving strategies and technologies. *Renew. Sustain. Energy Rev.* **2015**, *48*, 870–891, doi:10.1016/j.rser.2015.03.100.
6. Zhou, L.; Li, J.; Li, F.; Meng, Q.; Li, J.; Xu, X. Energy consumption model and energy efficiency of machine tools: A comprehensive literature review. *J. Clean. Prod.* **2016**, *112*, 3721–3734, doi:10.1016/j.jclepro.2015.05.093.
7. Zhou, L.; Li, J.; Li, F.; Xu, X.; Wang, L.; Wang, G.; Kong, L. An improved cutting power model of machine tools in milling process. *Int. J. Adv. Manuf. Technol*. **2017**, *91*, 2383–2400, doi:10.1007/s00170-016-9929-x.
8. Bayoumi, A.E.; Yücesan, G.; Hutton, D.V. On the closed form mechanistic modeling of milling: Specific cutting energy, torque, and power. *J. Mater. Eng. Perform.* **1994**, *3*, 151–158, doi:10.1007/BF02654511.
9. Draganescu, F.; Gheorghe, M.; Doicin, C.V. Models of machine tool efficiency and specific consumed energy. *J. Mater. Process. Technol.* **2003**, *141*, 9–15, doi:10.1016/S0924-0136(02)00930-5.
10. Gutowski, T.; Dahmus, J.; Thiriez, A. Electrical Energy Requirements for Manufacturing Processes. In Proceedings of 13th CIRP International Conference of Life Cycle Engineering, Lueven, Belgium, 31 May–2 June 2006; pp. 1–5.
11. Li, W.; Kara, S. An empirical model for predicting energy consumption of manufacturing processes: A case of turning process. *Proc. Inst. Mech. Eng. Part B J. Eng. Manuf.* **2011**, *225*, 1636–1646, doi:10.1177/2041297511398541.
12. He, Y.; Liu, B.; Zhang, X.; Gao, H.; Liu, X. A modeling method of task-oriented energy consumption for machining manufacturing system. *J. Clean. Prod.* **2012**, *23*, 167–174, doi:10.1016/j.jclepro.2011.10.033.
13. Li, L.; Yan, J.; Xing, Z. Energy requirements evaluation of milling machines based on thermal equilibrium and empirical modelling. *J. Clean. Prod.* **2013**, *52*, 113–121, doi:10.1016/j.jclepro.2013.02.039.
14. Li, T.; Yuan, C. Numerical Modeling of Specific Energy Consumption in Machining Process. In Proceedings of ASME 2013 International Manufacturing Science and Engineering Conference collocated with the 41st North American Manufacturing Research Conference, Madison, WI, USA, 10–14 June 2013.
15. Moon, J.-Y.; Shin, K.; Park, J. Optimization of production scheduling with time-dependent and machine-dependent electricity cost for industrial energy efficiency. *Int. J. Adv. Manuf. Technol.* **2013**, *68*, 523–535, doi:10.1007/s00170-013-4749-8.
16. Velchev, S.; Kolev, I.; Ivanov, K.; Gechevski, S. Empirical models for specific energy consumption and optimization of cutting parameters for minimizing energy consumption during turning. *J. Clean. Prod.* **2014**, *80*, 139–149, doi:10.1016/j.jclepro.2014.05.099.
17. O'Rielly, K.; Jeswiet, J. Strategies to Improve Industrial Energy Efficiency. *Procedia CIRP* **2014**, *15*, 325–330, doi:10.1016/j.procir.2014.06.074.
18. Zhao, G.; Hou, C.; Qiao, J.; Cheng, X. Energy consumption characteristics evaluation method in turning. *Adv. Mech. Eng.* **2016**, *8*, 1687814016680737, doi:10.1177/1687814016680737.
19. Sealy, M.P.; Liu, Z.Y.; Zhang, D.; Guo, Y.B.; Liu, Z.Q. Energy consumption and modeling in precision hard milling. *J. Clean. Prod.* **2016**, *135*, 1591–1601, doi:10.1016/j.jclepro.2015.10.094.
20. Hu, S.; Liu, F.; He, Y.; Hu, T. An on-line approach for energy efficiency monitoring of machine tools. *J. Clean. Prod.* **2012**, *27*, 133–140, doi:10.1016/j.jclepro.2012.01.013.
21. Mativenga, P.T.; Rajemi, M.F. Calculation of optimum cutting parameters based on minimum energy footprint. *CIRP Ann.* **2011**, *60*, 149–152, doi:10.1016/j.cirp.2011.03.088.
22. Behrendt, T.; Zein, A.; Min, S. Development of an energy consumption monitoring procedure for machine tools. *CIRP Ann.* **2012**, *61*, 43–46, doi:10.1016/j.cirp.2012.03.103.
23. Aramcharoen, A.; Mativenga, P.T. Critical factors in energy demand modelling for CNC milling and impact of toolpath strategy. *J. Clean. Prod.* **2014**, *78*, 63–74, doi:10.1016/j.jclepro.2014.04.065.

24. Guo, Y.; Duflou, J.R.; Qian, J.; Tang, H.; Lauwers, B. An operation-mode based simulation approach to enhance the energy conservation of machine tools. *J. Clean. Prod.* **2015**, *101*, 348–359, doi:10.1016/j.jclepro.2015.03.097.
25. Balogun, V.A.; Gu, H.; Mativenga, P.T. Improving the integrity of specific cutting energy coefficients for energy demand modelling. *Proc. Inst. Mech. Eng. Part B J. Eng. Manuf.* **2015**, *229*, 2109–2117, doi:10.1177/0954405414546145.
26. Altıntaş, R.S.; Kahya, M.; Ünver, H.Ö. Modelling and optimization of energy consumption for feature based milling. *Int. J. Adv. Manuf. Technol.* **2016**, *86*, 3345–3363, doi:10.1007/s00170-016-8441-7.
27. Albertelli, P.; Keshari, A.; Matta, A. Energy oriented multi cutting parameter optimization in face milling. *J. Clean. Prod.* **2016**, *137*, 1602–1618, doi:10.1016/j.jclepro.2016.04.012.
28. Ma, F.; Zhang, H.; Cao, H.; Hon, K.K.B. An energy consumption optimization strategy for CNC milling. *Int. J. Adv. Manuf. Technol.* **2017**, *90*, 1715–1726, doi:10.1007/s00170-016-9497-0.
29. Jia, S.; Yuan, Q.; Lv, J.; Liu, Y.; Ren, D.; Zhang, Z. Therblig-embedded value stream mapping method for lean energy machining. *Energy* **2017**, *138*, 1081–1098, doi:10.1016/j.energy.2017.07.120.
30. Chen, X.; Li, C.; Jin, Y.; Li, L. Optimization of cutting parameters with a sustainable consideration of electrical energy and embodied energy of materials. *Int. J. Adv. Manuf. Technol.* **2018**, *96*, 775–788, doi:10.1007/s00170-018-1647-0.
31. Fujishima, M.; Mori, M.; Oda, Y. Energy-efficient manufacturing on machine tools by machining process improvement. *Prod. Eng.* **2014**, *8*, 217–224, doi:10.1007/s11740-013-0492-0.
32. Mori, M.; Fujishima, M.; Inamasu, Y.; Oda, Y. A study on energy efficiency improvement for machine tools. *CIRP Ann.* **2011**, *60*, 145–148, doi:10.1016/j.cirp.2011.03.099.
33. Yan, J.; Li, L. Multi-objective optimization of milling parameters—The trade-offs between energy, production rate and cutting quality. *J. Clean. Prod.* **2013**, *52*, 462–471, doi:10.1016/j.jclepro.2013.02.030.
34. Kant, G.; Sangwan, K.S. Prediction and optimization of machining parameters for minimizing power consumption and surface roughness in machining. *J. Clean. Prod.* **2014**, *83*, 151–164, doi:10.1016/j.jclepro.2014.07.073.
35. Iqbal, A.; Zhang, H.-C.; Kong, L.L.; Hussain, G. A rule-based system for trade-off among energy consumption, tool life, and productivity in machining process. *J. Intell. Manuf.* **2015**, *26*, 1217–1232, doi:10.1007/s10845-013-0851-x.
36. Bilga, P.S.; Singh, S.; Kumar, R. Optimization of energy consumption response parameters for turning operation using Taguchi method. *J. Clean. Prod.* **2016**, *137*, 1406–1417, doi:10.1016/j.jclepro.2016.07.220.
37. Kumar, R.; Bilga, P.S.; Singh, S. Multi objective optimization using different methods of assigning weights to energy consumption responses, surface roughness and material removal rate during rough turning operation. *J. Clean. Prod.* **2017**, *164*, 45–57.
38. Teimouri, R.; Amini, S.; Lotfi, M.; Alinaghian, M. Sustainable drilling process of 1045 steel plates regarding minimum energy consumption and desired work quality. *Int. J. Lightweight Mater. Manuf.* **2019**, *2*, 397–406, doi:10.1016/j.ijlmm.2019.04.011.
39. Su, Y.; Zhao, G.; Zhao, Y.; Meng, J.; Li, C. Multi-Objective Optimization of Cutting Parameters in Turning AISI 304 Austenitic Stainless Steel. *Metals* **2020**, *10*, 217, doi:10.3390/met10020217.
40. Warsi, S.S.; Jaffery, H.I.; Ahmad, R.; Khan, M.; Akram, S. Analysis of power and specific cutting energy consumption in orthogonal machining of al 6061-T6 alloys at transitional cutting speeds. In Proceedings of ASME 2015 International Mechanical Engineering Congress and Exposition, IMECE 2015, Houston, TX, USA, 13–19 November 2015.
41. Bustillo, A.; Pimenov, D.Y.; Mia, M.; Kapłonek, W. Machine-learning for automatic prediction of flatness deviation considering the wear of the face mill teeth. *J. Intell. Manuf.* **2021**, *32*, 895–912, doi:10.1007/s10845-020-01645-3.
42. Khan, A.M.; Anwar, S.; Gupta, M.K.; Alfaify, A.; Hasnain, S.; Jamil, M.; Mia, M.; Pimenov, D.Y. Energy-Based Novel Quantifiable Sustainability Value Assessment Method for Machining Processes. *Energies* **2020**, *13*, 6144.
43. Singh, G.; Sharma, V.S.; Gupta, M.K.; Nguyen, T.-T.; Królczyk, G.M.; Pimenov, D.Y. Parametric optimization of multi-phase MQL turning of AISI 1045 for improved surface quality and productivity. *J. Prod. Syst. Manuf. Sci.* **2021**, *2*, 5–16.
44. Markopoulos, A.P.; Karkalos, N.E.; Mia, M.; Pimenov, D.Y.; Gupta, M.K.; Hegab, H.; Khanna, N.; Aizebeoje Balogun, V.; Sharma, S. Sustainability Assessment, Investigations, and Modelling of Slot Milling Characteristics in Eco-Benign Machining of Hardened Steel. *Metals* **2020**, *10*, 1650.
45. Jamil, M.; Zhao, W.; He, N.; Gupta, M.K.; Sarikaya, M.; Khan, A.M.; R, S.M.; Siengchin, S.; Pimenov, D.Y. Sustainable milling of Ti–6Al–4V: A trade-off between energy efficiency, carbon emissions and machining characteristics under MQL and cryogenic environment. *J. Clean. Prod.* **2021**, *281*, 125374, doi:10.1016/j.jclepro.2020.125374.
46. Pimenov, D.Y.; Abbas, A.T.; Gupta, M.K.; Erdakov, I.N.; Soliman, M.S.; El Rayes, M.M. Investigations of surface quality and energy consumption associated with costs and material removal rate during face milling of AISI 1045 steel. *Int. J. Adv. Manuf. Technol.* **2020**, *107*, 3511–3525, doi:10.1007/s00170-020-05236-7.
47. Karim, M.R.; Tariq, J.B.; Morshed, S.M.; Shawon, S.H.; Hasan, A.; Prakash, C.; Singh, S.; Kumar, R.; Nirsanametla, Y.; Pruncu, C.I. Environmental, Economical and Technological Analysis of MQL-Assisted Machining of Al-Mg-Zr Alloy Using PCD Tool. *Sustainability* **2021**, *13*, 7321, doi:10.3390/su13137321.
48. Kumar, R.; Singh, S.; Sidhu, A.S.; Pruncu, C.I. Bibliometric Analysis of Specific Energy Consumption (SEC) in Machining Operations: A Sustainable Response. *Sustainability* **2021**, *13*, 5617, doi:10.3390/su13105617.
49. Sen, B.; Gupta, M.K.; Mia, M.; Pimenov, D.Y.; Mikołajczyk, T. Performance Assessment of Minimum Quantity Castor-Palm Oil Mixtures in Hard-Milling Operation. *Materials* **2021**, *14*, 198.
50. Abbas, A.T.; Gupta, M.K.; Soliman, M.S.; Mia, M.; Hegab, H.; Luqman, M.; Pimenov, D.Y. Sustainability assessment associated with surface roughness and power consumption characteristics in nanofluid MQL-assisted turning of AISI 1045 steel. *Int. J. Adv. Manuf. Technol.* **2019**, *105*, 1311–1327, doi:10.1007/s00170-019-04325-6.

51. Markiewicz, H.; Klajn, A. Voltage disturbances standard en 50160-voltage characteristics in public distribution systems. *Wroc. Univ. Technol.* **2004**, *21*, 215–224.
52. Pimenov, D.Y.; Bustillo, A.; Mikolajczyk, T. Artificial intelligence for automatic prediction of required surface roughness by monitoring wear on face mill teeth. *J. Intell. Manuf.* **2018**, *29*, 1045–1061, doi:10.1007/s10845-017-1381-8.
53. Association, C.D. Voltage Disturbances. Standard EN 50160 Voltage Characteristics in Public Distribution Systems. In *Power Quality Application Guide*; European Copper Institute: Brussels, Belgium, 2004; pp. 7–21.
54. Anderson, M.J.; Whitcomb, P.J. *RSM Simplified*: *Optimizing Processes Using Response Surface Methods for Design of Experiments*; 2nd ed.; Taylor & Francis, CRC Press: Boca Raton, FL, USA, 2016; p. 311.
55. Zhang, S. Analysis of some measurement issues in bushing power factor tests in the field. *IEEE Trans. Power Deliv.* **2006**, *21*, 1350–1356, doi:10.1109/TPWRD.2006.874616.
56. Kumar, R.; Kaur, S. Multi Attribute Decision Making Approach to Select Microwave Oven with TOPSIS Method. In Proceedings of the 7th International Conference on Advancements in Engineering and Technology (ICAET-2019), Bhai Gurdas Institute of Engineering & Technology, Sangrur, India, 15–16 March 2019; pp. 357–361.
57. Kumar, R.; Dubey, R.; Singh, S.; Singh, S.; Prakash, C.; Nirsanametla, Y.; Królczyk, G.; Chudy, R. Multiple-Criteria Decision-Making and Sensitivity Analysis for Selection of Materials for Knee Implant Femoral Component. *Materials* **2021**, *14*, 2084, doi:10.3390/ma14082084.
58. Kumar, R.; Singh, S.; Bilga, P.S.; Jatin; Singh, J.; Singh, S.; Scutaru, M.-L.; Pruncu, C.I. Revealing the benefits of entropy weights method for multi-objective optimization in machining operations: A critical review. *J. Mater. Res. Technol.* **2021**, *10*, 1471–1492, doi:10.1016/j.jmrt.2020.12.114.
59. Chodha, V.; Dubey, R.; Kumar, R.; Singh, S.; Kaur, S. Selection of industrial arc welding robot with TOPSIS and Entropy MCDM techniques. *Mater. Today Proc.* **2021**, 10.1016/j.matpr.2021.04.487, doi:10.1016/j.matpr.2021.04.487.
60. Saaty, T.L. Decision making—The Analytic Hierarchy and Network Processes (AHP/ANP). *J. Syst. Sci. Syst. Eng.* **2004**, *13*, 1–35, doi:10.1007/s11518-006-0151-5.